STABILIZATION OF LANGMUIR AND LANGMUIR BLODGETT CETYLTRIMETHYLAMMONIUM BROMIDE MONOLAYERS BY GLUING WITH POLYSTYRENE SULFONATE

A THESIS SUBMITTED TO
THE GRADUATE SCHOOL OF NATURAL AND APPLIED SCIENCES
OF
MIDDLE EAST TECHNICAL UNIVERSITY

BY

NEZAKET NEHIR UTKU

IN PARTIAL FULFILLMENT OF THE REQUIREMENTS
FOR
THE DEGREE OF MASTER OF SCIENCE
IN
POLYMER SCIENCE AND TECHNOLOGY

FEBRUARY 2015

Approval of the thesis:

STABILIZATION OF LANGMUIR AND LANGMUIR BLODGETT CETYLTRIMETHYLAMMONIUM BROMIDE MONOLAYERS BY GLUING WITH POLYSTYRENE SULFONATE

submitted by **NEZAKET NEHIR UTKU** in partial fulfillment of the requirements for the degree of **Master of Science in Polymer Science and Technology Department, Middle East Technical University** by,

Prof. Dr. Gülbin Dural Ünver _____
Dean, Graduate School of **Natural and Applied Sciences**

Prof. Dr. Necati Özkan _____
Head of Department, **Polymer Science and Technology**

Prof. Dr. Erdal Bayramlı _____
Supervisor, **Chemistry Department, METU**

Prof. Dr. Mürvet Volkan _____
Co-supervisor, **Chemistry Department, METU**

Examining Committee Members:

Prof. Dr. Necati Özkan _____
Polymer Science and Technology Department, METU

Prof. Dr. Erdal Bayramlı _____
Chemistry Department, METU

Prof. Dr. Mürvet Volkan _____
Chemistry Department, METU

Prof. Dr. Cevdet Kaynak _____
Materials and Metallurgical Engineering Department, METU

Assoc. Prof. Dr. Ali Çırpan _____
Chemistry Department, METU

Date: 06.02.2015

I hereby declare that all information in this document has been obtained and presented in accordance with academic rules and ethical conduct. I also declare that, as required by these rules and conduct, I have fully cited and referenced all material and results that are not original to this work.

Name, Last Name: Nezaket Nehir UTKU

Signature:

ABSTRACT

STABILIZATION OF LANGMUIR AND LANGMUIR BLODGETT CETYLTRIMETHYLAMMONIUM BROMIDE MONOLAYERS BY GLUING WITH POLYSTYRENE SULFONATE

Utku, Nezaket Nehir
M. S., Department of Polymer Science and Technology
Supervisor: Prof. Dr. Erdal Bayramlı
Co-Supervisor: Prof. Dr. Murvet Volkan
February 2015, 102 pages

Organic thin films have wide range application areas such as biosensors, permeation selective barriers, molecular electronics, optical devices and coatings. The properties of such films can be tuned by their composition, structure and uniformity. Stability of obtained films has also an important factor in the fabrication and the transfer of the films. For this aim, Langmuir is an elegant technique for both the production and deposition of monolayers onto a solid support.

Herein, some optimization studies such as subphase temperature, pH, compression rate and transfer rate were performed with stearic acid (SA) and octadecane-1-thiol (ODT) which are the standard materials of Langmuir system. Concentration and subphase temperature were also optimized for cetyltrimethylammonium bromide (CTAB) which was used to prepare and organize the gold nanorods (GNRs) in a monolayer structure. Lately, it was reported that some water soluble materials can also form Langmuir monolayers but to produce a Langmuir compatible complex, an interaction with these water soluble materials with a water insoluble material is

needed. However, CTAB was used by itself without any complex forming reagent and stable monolayers were obtained.

Polymers, particularly water soluble ones, are used as a glue to improve the cohesiveness of LB films. This process is known as “gluing” where LB assemblies were cross-linked noncovalently through ionic and hydrophobic association with a water-soluble polymers.

The effect of gluing on stability of CTAB monolayers was investigated. Poly(4-styrenesulfonate) (PSS) was used as a gluing agent.

The addition of polymers into subphase led to an interaction between surfactant and polyelectrolyte and an increase in monolayer stability. In order to compare the effect of PSS on stability of the obtained monolayers, hysteresis loops (repeatedly compression-expansion cycles) were performed in the presence and absence of PSS in the subphase and it was concluded that more stabilized CTAB monolayers can be obtained by gluing. Moreover, glued CTAB multilayers can be prepared by Langmuir Blodgett technique.

GNRs were synthesized by seed mediated growth approach. The aspect ratio of the rods were approximately 2.5. The characterization of GNRs was performed by UV spectrometry. Two characteristic rod plasmon absorptions were observed at 520 and 675 nm. The morphology of the GNRs was characterized by Scanning Electron Microscopy (SEM).

After the deposition of negatively charged PSS glued CTAB monolayers, they were used for assembling the cationic gold nanorods on the surface of the substrate. Finally, the performance of the obtained structures as Surface Enhanced Raman Scattering (SERS) substrates were investigated utilizing brilliant cresyl blue (BCB) dye as a model compound.

Keywords: Langmuir, Gluing, Monolayer, Organic Thin Films, CTAB, Gold Nanorod, Polystyrene Sulfonate

ÖZ

LANGMUIR VE LANGMUIR BLODGETT SETİLTRİMETİLAMONYUM BROMÜR TEKLİKATMANLARININ POLİSTİREN SÜLFONAT İLE STABİLİZASYONU

Utku, Nezaket Nehir
Yüksek Lisans, Polimer Bilimi ve Teknolojisi Bölümü
Tez Yöneticisi: Prof. Dr. Erdal Bayramlı
Ortak Tez Yöneticisi: Prof. Dr. Mürvet Volkan
Şubat 2015, 102 sayfa

Organik ince filmler, biosensörler, seçici geçirgen bariyerler, moleküler elektronikler, optik cihazlar ve kaplamalar gibi geniş uygulama alanlarına sahiptirler. Bu filmlerin özellikleri, onların içerik, yapı ve bir örnekliklerine bağlı olarak değişiklik gösterir. Elde edilen bu filmlerin kararlılıkları, filmleri oluştururken ve özellikle transfer ederken, büyük önem taşır. Bu amaçla Langmuir, hem bu filmlerin üretiminde, hem de teklikatmanların katı bir destek üzerine transferinde benzersiz bir metod niteliğindedir.

Bu çalışmada, altfaz sıcaklığı, pH, sıkıştırma hızı ve transfer hızı gibi parametrelerin optimizasyon çalışmaları, Langmuir sisteminin standart materyalleri olan stearik asit (SA) ve oktadekan-1-tiol (ODT) ile gerçekleştirilmiştir. Derişim ve altfaz sıcaklığı, altın nanoçubukların teklikatman yapısında hazırlanması ve organize edilmesinde kullanılan setiltrimetilamonyum bromür (CTAB) için de optimize edilmiştir.

Son zamanlarda yapılan çalışmalarda, suda çözünen materyallerin de, Langmuir teklikatmanları oluşturabildiği ancak bunun için, suda çözünen ve çözünmeyen

amfifiller arasında bir etkileşimin gerekliliği vurgulanmaktadır. Bizim çalışmamızda, CTAB bir kompleks oluşturulmaksızın tek başına kullanılmış ve kararlı teklikatmanlar elde edilebilmiştir.

Polimerler, özellikle de suda çözünür olanlar, LB filmlerinin yapışkanlığını arttıran yapıştırıcılar olarak kullanılmaktadır. "Yapıştırma" olarak bilinen bu yöntemde, LB dizilimi, suda çözünür polimerlerle, kovalent bağlar kurmadan iyonik ve hidrofobik birleşmelerle çapraz bağlanır.

Yapıştırma tekniğinin, CTAB teklikatmalarının kararlılığına olan etkisi incelenmiştir. Poli(4-stirensülfonat) (PSS) yapıştırıcı madde olarak kullanılmıştır.

Altfaza eklenen polimer, yüzey aktif madde ve polielektrolitin kendisi arasında etkileşime neden olur ve teklikatmanın stabilizasyonunu arttırır. PSS`in, elde edilen teklikatmanların kararlılığına olan etkisini karşılaştırmak için, histerezis (tekrarlı sıkıştırma-açma) hareketlerinden yararlanılmış ve yapıştırma yöntemi ile daha kararlı CTAB teklikatmanları elde edilebildiği görülmüştür. Daha da önemlisi, Langmuir Blodgett tekniği ile yapışmış çoklukatmanlar hazırlanabileceği sonucuna varılmıştır.

Altın nanoçubuklar çekirdek ortamında büyütme (seed mediated growth) yaklaşımı ile sentezlenmiştir. Çubukların en-boy oranı, yaklaşık olarak 2.5'tur. Altın nanoçubukların karakterizasyonu, UV spekrometrisi ile gerçekleştirilmiştir. Nanoçubukların ayırt edici özelliği olan iki plazmon absorbsiyonu, 520 ve 675 nm'lerde gözlemlenmiştir. Altın nanoçubukların morfolojileri taramalı elektron mikroskobuyla (SEM) karakterize edilmiştir.

Negatif yüklü PSS ile yapıştırılmış, CTAB teklikatmanlarının katı yüzeye transfer edilmesinin ardından, teklikatmanlar, artı yüklü altın nanoçubukların katı yüzey üzerinde diziliminde kullanılmışlardır. Son olarak, elde edilen yapıların, parlak krezil mavisi (BCB) boyasının örnek bileşiğinden faydalanarak, Yüzeyde Güçlendirilmiş Raman Spektroskopisinde (SERS) performansı araştırılmıştır.

Anahtar kelimeler: Langmuir, Teklikatman, Organik İnce Filmler, CTAB, Altın Nanoçubuk, Polistiren sülfonat

to memory of my dad...

ACKNOWLEDGEMENTS

Firstly, I would like to thank my supervisor, Prof. Dr. Erdal BAYRAMLI, for his unique knowledge and guidance.

I want to thank my co-advisor Prof. Dr. Mürvet VOLKAN for her endless guidance, support and mostly encouragement. I have learned everything that I know during last two and a half year from her.

I would like to thank Murat KAYA for his valuable knowledge. He always came for me anytime when I needed.

I owe my thanks Ufuk ÖZGEN, for teaching me everything that I know about Langmuir. It was really an excellent experience for me working with him and learning how to think in chemistry.

I would like to give my special thanks Yeliz AKPINAR not only for her helps in every step of my study, but also her unique understanding, support and patience whenever I felt hopeless. Without her encouragement, I wouldn`t complete anything.

I want to thank Ceren UZUN for her contributions on the synthesis of gold nanorods and also her friendship.

I want to express my appreciation Dilek ÜNAL and Tayfun TAŞ for their friendship and cheerful lab environment.

I also want to thank C-49 lab members Emrah Yıldırım, Selin Bora, Pınar Akay Mercan, Başak and Sezin for their helps, friendship and funny activities.

I cannot explain my feelings about Melis, Esra ÖZ., Esra ÖĞ, Büke and Seza with just few words. They deserved the biggest thanks being with me during my whole university life. Anytime I need, they were ready for me. They will always be my best friends forever because there is nothing better than having a great family like that.

I also want to thank Merve and Ebru for their support and friendship. With the presence of them, my family is larger now.

I would like to give my special thanks Özge KOÇER for her endless friendship. Even if we are not together, I know that there is someone who is always thinking of me.

I owe my great thanks Özge, Ulaş, Akın and Gizem for their friendship and support for 13 years. It is priceless that whenever I remember a memory, they were certainly a part of it.

I also want to thank Mancar (Ali), Baki, Kübra and Gökmen for enjoyable times. I always felt happy when I was together with them.

I would like to thank my mother Selma and my sister Çisem for everything. My mom is the strongest woman that I know and it is a change being her daughter. My sister will always be my best friend and my idol rest of my life. She supported me always for my every decision. I cannot even think that I do not have her. I appreciate their existence.

Finally, I would like to thank Burak for his love, trust, support and patience. Whenever I felt sad, he always made me laugh. The only thing that I learned: I am the luckiest person in the world because I could find him.

TABLE OF CONTENTS

LIST OF FIGURES

FIGURES

LIST OF TABLE

TABLES

LIST OF EQUATIONS

EQUATIONS

LIST OF ABBREVIATIONS

ºC	degrees Celsius
Å	angstrom
µL	microliter
π	pressure
A	area
BCB	brilliant cresyl blue
cmc	critical micelle concentration
CTAB	cetyltrimethylammoniumbromide
CTMS	chlorotrimethylsilane
DI	deionized
GNR	gold nanorod
L	layer
LB	Langmuir-Blodgett
M	molar
mg	milligram
mg/mL	miligram per mililiter
mL	milliliter
mm	milimeter
mM	milimolar
MMA	mean molecular area
mm/min	millimeter per minute
mmol	millimole
mN/m	milinewton per meter
nm	nanometer
ODT	octadecane-1-thiol
PSS	polystyrenesulfonate

rpm	round per minute
SA	stearic acid
SEM	Scanning Electron Microscopy
SERS	Surface Enhanced Raman Scattering
TR	transfer ratio
UV-Vis	Ultraviolet-Visible

CHAPTER 1

INTRODUCTION

1.1. Langmuir and Langmuir Blodgett Films

1.1.1. History of Langmuir Films

The first idea of manipulation of oil films on water surface was produced by Agnes Pockels at 1891 while she was working in her kitchen and right after; Lord Rayleigh at 1899 supplied foundation for experiments with insoluble monolayers on water surface[1]. Further experimental methods enabled Devaux to measure the thickness of the films and Hardy to discover that oils cannot be spread over the water surface without polar functional groups[2]. In 1917, Irving Langmuir carried out lots of new methods with amphiphilic molecules at the air-water interface and became the father of the field with his unique contributions to the surface chemistry. He improved a device which measures the forces on deflection of the films and also verified that the polar heads of the amphiphilic molecules immersed into water while nonpolar chains positioned at air phase. In addition to that, Langmuir had a great contribution to literature about which amphiphiles produces stable monolayer films[3]. With the help of guidance of Langmuir, Katherine Blodgett performed the transfer of fatty acid monolayers onto a solid support. Related studies on the subject were covered by Gaines and Barnes near the end of the twentieth century[4].

LB films have many possible applications fundamentally in technological and biological areas especially with the chance of producing them with various materials such as polymers, nanomaterials and other amphiphiles also. They can be used as sensors, diodes and transistors in electronic and optical devices[5], catalysts and lubricants in chemistry[6] and biosensors in medicine[7]. Langmuir-Blodgett is a wondrous technique to obtain one molecule thick monolayers and multilayers with various materials at different interfaces and to transfer of them onto desired substrate by organizing the materials in a highly controllable way.

1.1.2. Theory of Langmuir and Langmuir Blodgett Films

1.1.2.1. Self-Assembled Monolayers

Self-assembled monolayers can be defined as organized structures that produced spontaneously with the affinity of functional groups toward substrate or patterned material without any external force. The process can be performed mainly in two ways; by physisorption or by chemisorption. When these are compared, chemisorption leads a more stable binding due to stronger intermolecular forces between adsorbate and substrate including hydrogen bonding, donor–acceptor and ion pairing[8]. For instance, monolayers of thiol terminated groups on gold surface can be accepted as a good example for the self-assembly with their high affinity to form strong sulfur-gold interaction. This high affinity enables to use these thiol terminated self-assembled monolayers in molecular electronic device applications[9].

1.1.2.2. Bulk Phases

There exist three common states of matter which are gas, liquid and solid. These three phases differ from each other by degree of orientational and translational order of the molecules. In the gaseous state, the molecules have very weak intermolecular forces so they can move almost freely in the container they occupy. In the liquid phase, intermolecular forces between liquid molecules are relatively stronger compared to the gas and molecules have also random motion. The solid state of matter, molecules have the strongest forces and correspondingly distance between the molecules is very small and they have rigid arrangement. For the solid phase, there exist two more subclasses; crystalline (patterned arrangement) and amorphous (no pattern in arrangement). Transitions between the states may occur by changing the conditions of the medium such as temperature or pressure[5].

1.1.2.3. Interfaces

Interfaces are defined as the regions where two homogeneous bulk phases intersect. Properties of the interfaces significantly change while moving from one phase to other. They can be classified under five main titles according to the states of bulks which are represented in Table 1.1[4].

Table 1. 1 Classification of interfaces

fluid interfaces	**non-fluid or solid interfaces**

Table 1. 1 (continued)

gas – liquid G – L	gas – solid G – S
liquid 1 – liquid 2 $L_1 – L_2$	liquid – solid L – S
	solid 1 – solid 2 $S_1 – S_2$

When it is looked closely at a gas-liquid interface, for instance air-water interface, it is obvious that, there exist the gaseous properties of air which exhibits collisions of molecules with random motion while removing from the water surface. On the other hand, below the water surface, molecules are relatively close packed due to strong intermolecular forces, in this case mainly hydrogen bonding, and so they have restricted freedom which was illustrated in Figure 1.1.

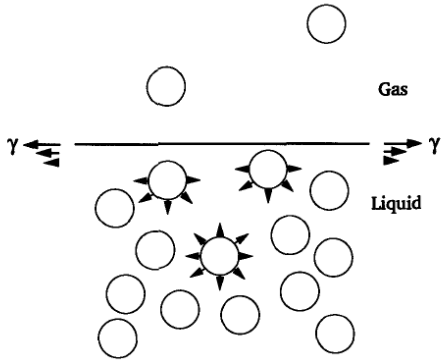

Figure 1. 1 Schematic representation of forces between molecules both in the bulk and the interface[6]

1.1.2.4. Surface Active Agents

If it is necessary to classify all compounds, they can be separated in two general groups; water soluble compounds and water insoluble compounds. Water soluble ones usually have polar nature which means having an electric dipole moment in the compound. On the other hand, water insoluble molecules are called mostly nonpolar and they have zero dipole moment. For the fabrication of Langmuir monolayers, molecules having amphiphilic character can be used. An amphiphilic molecule (surfactant) has both a polar (hydrophilic) part and nonpolar (hydrophobic) long chain. Figure 1.2 represents the components of an amphiphile.

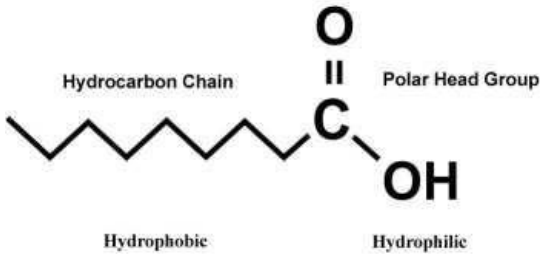

Figure 1. 2 Components of an amphiphile[5]

This nature of surfactants enables the polar group to dissolve in water while the nonpolar chain points toward the air state and so, two hydrophilic and two hydrophobic interfaces lowers the total energy of the system compared with the initially higher energy interface. Therefore, amphiphiles generally have the tendency to orient normal to the surface with forming one molecule thickness[10].

Today Langmuir is a very applicable technique for many different materials such as fatty acids, dyes, complexes, polymers, biological compounds and nanostructures to organize them in molecular level for desired applications[5].

1.1.2.5. Surface Tension and Surface Pressure

Surface tension has a great importance for the interfaces with excess energy it represents because of the different nature of molecules at surface and in the bulk. This extra energy increases proportionally with the surface area[4]. Figure 1.3 shows the forces at the surface and in the bulk.

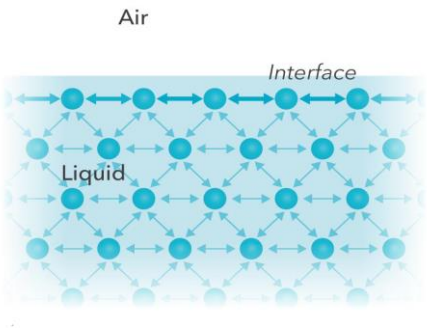

Figure 1. 3 Balanced and unbalanced forces both near and at the surface[4]

In some cases, for instance, one side of the molecule prefers to stay one phase while the other side stays the other phase or fabrication of an insoluble monolayer on a liquid surface, generally surface pressure term is used. So the surface pressure can be explained as the decrease in the surface tension of the liquid with the presence of the monolayer on it[11]. The equation that defines the relationship between surface tension and surface pressure can be represented as equation 1.1.

$$\boldsymbol{\Pi = \gamma - \gamma_o} \qquad \textit{1. 1}$$

γ defines the surface tension at the absence of the monolayer, and γ_o defines the surface tension at the presence of the monolayer[5]. Water has 73 mNm^{-1} surface tension value at 20 $^{\circ}C$ and atmospheric pressure. The answer of the why water is mostly used subphase is its exceptionally higher surface tension value compared to other liquids[3].

1.1.2.6. Insoluble Monolayers

In order to produce monolayers, lots of different materials were studied up till now. All of these materials can be roughly classified in two groups; nonpolymeric substances which are already insoluble but have enough tendency to the subphase with spreading property on the liquid surface including long-chain fatty acids and alcohols with polar –COOH or –OH groups and polymeric substances such as some proteins and synthetic polymers which can be positively adsorbed at the interface[6]. Table 1.2 summarizes the strength of the produced monolayers of different compounds.

Table 1. 2 Stability of monolayers having different functional groups

Very weak (no film)	**Weak** (unstable films)	**Strong** (stable film with C_{16} chain)	**Very strong** (C_{16} chain compounds dissolve)
Hydrocarbon	$-CH_2OCH_3$	$-CH_2OH$	$-SO_3^-$
$-CH_2I$	$-C_6H_4OCH_3$	-COOH	$-OSO_3^-$
$-CH_2Br$	$-COOCH_3$	-CN	$-C_6H_4SO_4$
$-CH_2Cl$		$-CONH_2$	$-NR_3^+$
$-NO_2$		-CH=NOH	
		$-C_6H_4OH$	

Table 1. 2 (continued)

		$-CH_2COCH_3$	
		$-NHCONH_2$	
		$-NHCOCH_3$	

In order to organize compounds on a liquid surface, firstly they should be dissolved into an insoluble and volatile solvent because after the evaporization of the solvent, remaining molecules on the surface can be compressed to obtain an ordered, solid like monolayer. The different nature of the two ends of the molecules lead to same alignment with each other.

Main target of the thermodynamic systems is always to reach equilibrium state and it can be succeeded by reducing the free energy. To minimize free energy, either the internal energy should be reduced or entropy should be increased[5].

1.1.2.7. Monolayers of Water Soluble Materials

As it was explained before, the most appropriate materials in the use of Langmuir technique are insoluble amphiphiles which are composed of a polar head and a long nonpolar chain. However recently, highly organized monolayers can also be obtained with lightly substituted water soluble (nonamphiphilic) materials such as anionic or cationic surfactants at the air-water interface. But in this case, there exists a

requirement that, these water soluble substances should interact with some insoluble materials like long chain fatty acids or inert polymers to get a Langmuir compatible structure[12–15]. The use of the water soluble materials also on Langmuir technique allows them to orientate and organize as monolayers and multilayers on different solid surfaces with tunable physical, chemical and optical properties according to desired applications[16,17].

1.1.2.8. Surface Film Balance

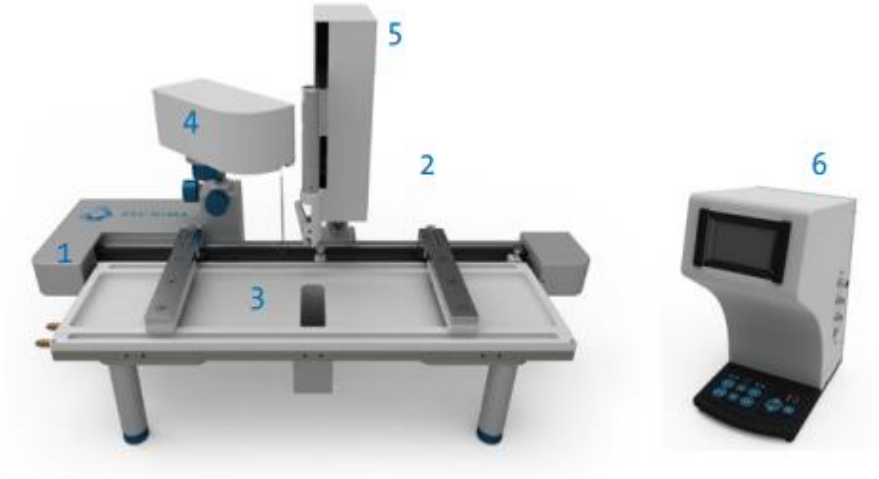

Figure 1. 4 Parts of Langmuir device (1 frame, 2 barriers, 3 trough top, 4 surface pressure sensor, 5 dipping mechanism, 6 interface unit)[18]

Figure 1.4 shows the main parts of Langmuir instrument. Monolayers of surfactants are mainly obtained on surface film balance in other words Langmuir trough which is formed with a hydrophobic material. On the trough, there exist movable hydrophilic barriers and a Wilhelmy plate that measures the surface tension hanging partially into the subphase. Trough is filled with subphase generally with water that the monolayer of the desired material obtained on it. When the barriers are fully open, subphase insoluble, volatile solution of surfactant is spread over the subphase at defined concentration and volume and then, after the evaporation of solvent, barriers close to each other producing monolayer. The area covered by monolayer is also known; therefore, area per molecule can be calculated by equation 1.2.

$$\mathbf{A_M = A / N_M} \qquad \textit{1. 2}$$

which **A** is the area of the surface occupied by monolayer and $\mathbf{N_M}$ is the surfactant amount loaded on subphase surface. So with the help of this equation, average area of per molecule of the monolayer can be calculated[4].

While a monolayer is producing, both the surface pressure and mean molecular area are monitored. Surface pressure is determined by Wilhelmy plate which is exposed to force caused by surface tension. Due to the dimensions of the plate are known, the force measured then converted into surface tension value in mN/m or dynes/cm units. Simultaneously, mean molecular area is measured by the instant distance between barriers and dimensions of the trough.

Wilhelmy plate is mostly made of pure platinum but other different materials such as glass or paper can also be used. There are three forces that plate exposed to which are gravitational force, the force caused by surface tension at downward and buoyancy force of water at the opposite direction. The net force is determined by the equation 1.3.

$$F = \boldsymbol{\rho_p g l_p w_p t_p + 2\gamma\left(t_p w_p\right)(\cos\theta) - \rho_l g t_l w_l h_l} \qquad \textit{1.3}$$

where l_p, w_p and t_p are dimensions and ρ_p is density of the plate, h_l is the depth of the plate immersed into the subphase, ρ_l is the density, γ is surface tension of the liquid subphase, θ is the contact angle of the liquid on the plate and g is the gravitational constant. The force is measured then converted into surface pressure by measuring the difference at the presence and the absence of the monolayer. The surface pressure is calculated by equation 1.4 and if the Wilhelmy plate is completely immersed into the subphase (i.e. $\cos\theta = 1$).

$$\boldsymbol{\Pi = -\Delta\gamma = -\left[\Delta F / 2\left(t_p + w_p\right)\right] = -\Delta F / 2w_p, if\ w_p \gg t_p} \qquad \textit{1.4}$$

Sensitivity of the measurement depends inversely on the thickness of the plate so if the thickness of the plate decreases, the sensitivity increases[4].

1.1.2.9. Surface Pressure-Area Relationships and Phase Transitions

Main data obtained from the Langmuir experiments are surface pressure versus mean molecular area isotherms as represented in Figure 1.5. By monitoring the instant changes of surface pressure against area, phase transitions that mostly consists of gaseous (G) phase, a liquid-expanded (Le or L_1) phase, a liquid-condensed (Lc or L_2) phase, and solid (S) phase are observed.

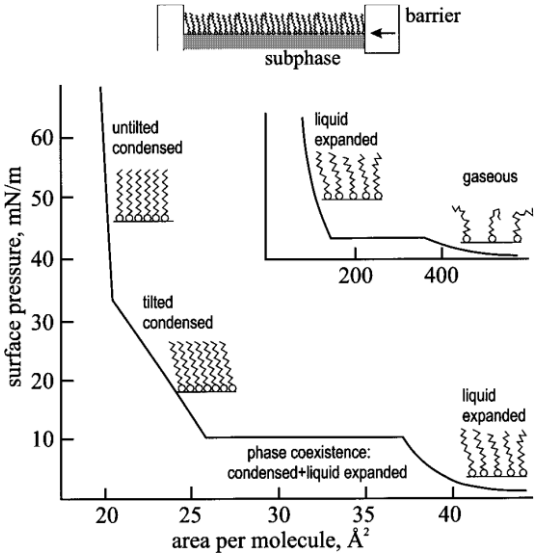

Figure 1. 5 Surface pressure versus area per molecule isotherm for a long- chain organic compound[12]

Initially at the gaseous state, molecules are quite far from each other and by compressing, the distance between them are decreased and the liquid-expanded and liquid-condensed states are observed respectively. In the liquid-expanded phase, while the hydrophilic heads are translationally disordered, long hydrophobic chains are disordered conformationally. Transition from liquid expanded to liquid-condensed phase is a first-order transition although the first-order transitions should be observed at constant pressure regions and for many isotherms; transitions are not completely horizontal plateau[19]. These nonhorizontal regions can be theoretically explained with the existence of small aggregates and micelles on the surface[20,21]. Finally keeping compression, molecules highly close to each other and become less compressible and 2-dimensional solid like monolayer is obtained. A second-order transition shows a striking change in the slope and occurs from liquid-condensed to solid state[4].

1.1.3. Deposition of Langmuir Blodgett Films

Obtained Langmuir monolayers at the interface can be transferred onto different solid supports via two main complementary methods which are Langmuir-Blodgett (vertical deposition) and Langmuir-Schaefer (horizontal deposition). In the former method, solid substrate is dipped into the subphase vertically when the stable deposition conditions which is solid phase surface pressure is reached and in the later one, the process is carried out by closing the substrate horizontally to the monolayer surface. Surely, optimum surface pressure for the deposition varies depending on the type of surfactant although there exists a limitation for the surface pressure which should have a value between 10 - 40 mN/m due to difficulties related with the collapse and rigidity of the monolayers. Langmuir Blodgett and Langmuir Schaefer methods were illustrated in Figure 1.6.

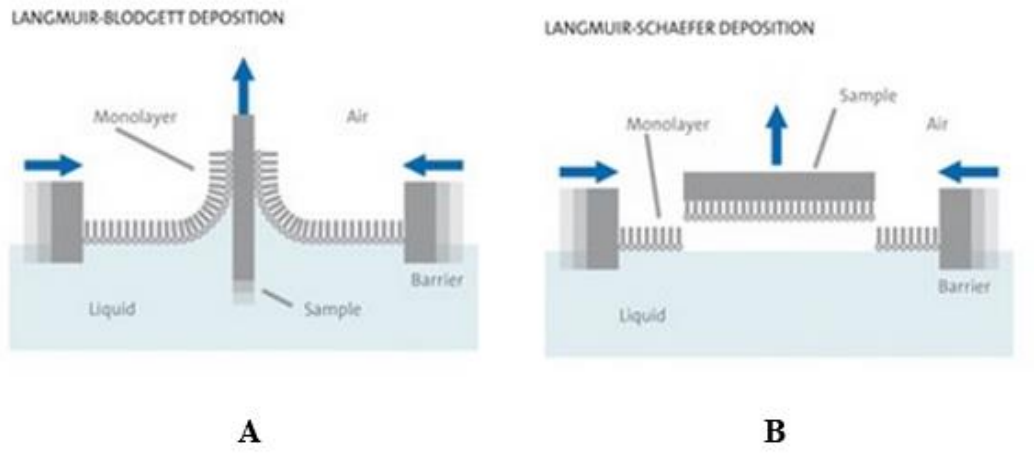

Figure 1. 6 Vertical and horizontal depositions of Langmuir monolayers (**A** Langmuir Blodgett, **B** Langmuir Schaefer)[18]

Surface modifications should be performed in order to transfer the monolayer from surface of subphase to the substrate. For this aim, according to the desired direction of the amphiphiles, hydrophilic or hydrophobic treatments can be done to the surface of the substrate and so different types of multilayers can be obtained represented as Figure 1.7.

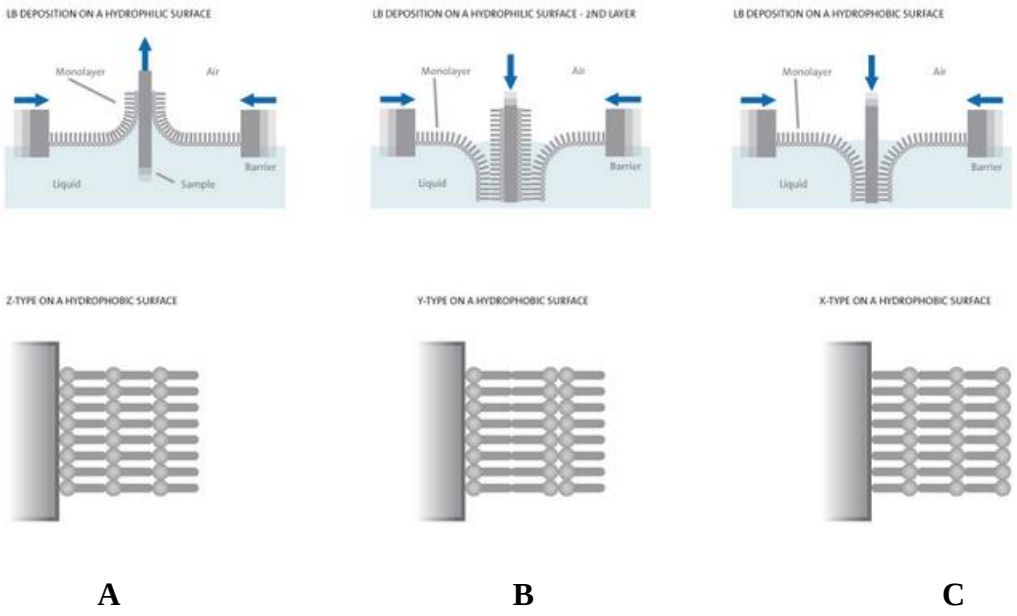

Figure 1. 7 Different types of Langmuir Blodgett multilayers (**A** Z-type, **B** Y-type, **C** X-type)[18]

In Langmuir-Blodgett type of transfer, to produce X-type of multilayer, hydrophobic substrate is prepared. When the monolayer is obtained at a specific surface pressure at the surface, the substrate is immersed into the subphase with a certain rate as the

barriers get closer to keep the molecules as monolayer form. After first layer is transferred the barriers are opened until surface pressure drops to zero and the solid support is withdrawn. The process is repeated up to desired numbers of layer is deposited. At the end, multilayer which composes of all tails are toward substrate while all hydrophilic heads are toward the opposite direction of the substrate. For the case of Z-type multilayer, firstly the hydrophilic substrate is prepared and before formation of the monolayer, support should be dipped into the subphase. Then, at the surface, the monolayer is formed and the substrate is withdrawn. In this time, for the transfer of each layer, before preparing the monolayer on the surface, substrate should be dipped into the subphase. Lastly for the Y-type of multilayers, repeated dipping and withdrawing cycles are performed. In the preparation of all types of multilayers, waiting time after each layer is transferred should be optimized.

The efficiency of the transfer can be defined by a value called as transfer ratio. The transfer ratio equals to the decreasing area of monolayer on surface of subphase over monolayer capped area of support. So, for an appropriate deposition, the transfer ratio should be close to 1[4].

Easy transfer of obtained monolayers from the surface to the substrate in a highly controlled way becomes a unique tool for plenty of applications in different fields. To get data for many processes such as wettability or friction determinations, gas permeation and membrane properties, Langmuir and related deposition methods provides great opportunities for the researchers[6].

1.1.4. Applications of Langmuir

Langmuir technique is a unique tool to organize and to orientate the materials in a molecular level. Since the properties of such materials directly depend on their organization, Langmuir film formation has a great importance for many applications.

Studies of Langmuir Blodgett films are usually conducted with some appropriate amphiphiles, such as fatty acids. However, in order to control the organization of thin films, polymers especially having low molecular weight are also good candidates for LB method. Since they have high thermal and mechanical stabilities, polymers can be used for tuning their molecular ordering[22–24]. Moreover, polymers, particularly water soluble ones, are used as a glue to improve the cohesiveness of LB films. This process is known as `gluing` where LB assemblies were cross-linked noncovalently through ionic and hydrophobic association with a water-soluble polymers[25–31]. Gluing is also very helpful to minimize the formation of defects within polymer monolayers and bilayers to give higher quality thin films through LB method[27]. For example, Regen and his coworkers proposed a strategy in order to design a selective gas membranes by utilizing gluing technique to change the barrier capabilities of LB films changing the thickness of the bilayers of calix-arene surfactants, they compared the N_2, He and CO_2 gas selectivity of glued and unglued ones. The study proved that there occurs an improvement of the gas selection when the bilayers were glued.

LB technique also provides a great opportunity for the applications of molecular electronics particularly to provide directional electron transfer, in usage as organic conductors, diodes and transistors[3]. Because the main requirement for the aforementioned devices is the assembly of the molecules. Likewise most of the novel applications in the areas of photonics, catalysis, sensors, and biomaterials are based on the assembly of nanoparticles into uniform thin films, with precise control over chemical and physical properties. Langmuir- Blodgett technique[32,33] is used for the deposition of nanoparticle monolayers on various substrates to create robust thin films of nanoparticles.

There are mainly two approaches for the deposition of nanoparticles. If the particles are charged, deposition generally includes immobilization of oppositely charged colloidal nanoparticles present in the subphase onto a charged amphiphilic Langmuir monolayer[34]. The driving force is the strong electrostatic interaction. Octadecylamine is usually employed for this purpose[35]. If the nanoparticles are hydrophobic then, they are dissolved in an organic solvent and then spread onto aqueous medium to form Langmuir monolayers of these particles[36,37]. These hydrophobic materials can be used in raman spectroscopy. Yang and coworkers applied LB technique to produce nanostructure monolayers in the preparation of surface enhanced raman scattering (SERS) substrate having high enhancement factors [38–41].

1.1.5. Aim of Study

There are three aims of this study: First to see the effect of gluing approach utilizing PSS, a soluble polymer as a glue, on the construction of CTAB monolayer by Langmuir method. The formed monolayer is expected to exhibit greater robustness during transformation onto the substrate. Second, we want to obtain a gold nanorod assembly using LB technique. For this purpose two strategies will be applied. In one of them we will examine the possibility of using this negatively charged PSS glued CTAB layers for assembling the cationic gold nanorods on the surface of the substrate. In the other method, hydrophobic gold nanorods will be dispersed in an organic solvent and then spread onto air- water interface to form Langmuir monolayer of the nanorods. Third was related with application. The gold nanorods coated surfaces will be utilized as a SERS substrate. To reach these goals, all the parameters of the LB system will be examined thoroughly using stearic acid and octadecane-1-thiol which are mostly studied and well characterized amphiphiles in LB system. Hysteresis experiments will be performed following the gluing process to

investigate the improvement of the stabilization of CTAB layer. The positively charged gold nanorods will be synthesized via seed mediated method where CTAB is used to stabilize the particles. A surface modification will be applied to cationic nanorods to render them hydrophobic.

CHAPTER 2

EXPERIMENTAL

2.1. Materials

Silver nitrate ($AgNO_3$, ≥ 99.0%), hexadecyltrimethylammoniumbromide (CTAB, 99%), hexane (≥ 95%), sodium borohydride ($NaBH_4$, ≥ 95% , hydrochloric acid (HCl, ≥ 37%), poly(4-styrenesulfonate) (PSS, 30 wt % in H_2O, av. MWt : 70000), brilliant cresyl blue (BCB), acetone (C_2H_6O, ≥ 99%) and gold (III) chloride trihydrate ($HAuCl_4.3H_2O$) were purchased from Sigma-Aldrich. 1-octadecanethiol (ODT, ≥ 95%) was provided from Fluka. Sodium borohydride ($NaBH_4$, ≥ 96%), hydrogenperoxide (H_2O_2, 35%), ammonia (25%), cholorotrimethylsilane (CTMS, ≥ 99%), ethanol, L(+)-ascorbic acid and stearic acid were purchased from Merck. Chloroform (CHCl3, 99%) was purchased from LabScan and deionized water (TKA deionizer, Germany) was used in all the experiments.

2.2. Instrumentation

2.2.1. UV-VIS Spectrometer

In order to determine the optical properties of gold nanorods (GNR), T80 double beam spectrometer which was manufactured by PG Instruments, UK equipped with socket deuterium and tungsten halogen lamp and multiplier detector was used.

2.2.2. Centrifuge

Sigma 2-16 centrifuge (max rotating speed: 13500 rpm) was used to separate and concentrate the GNRs in solution.

2.2.3. Surface Enhanced Raman Spectrometer (SERS)

LabRAM HR Raman spectrometer was used for SERS results to compare the BCB peak results. The instrument was manufactured by Jobin Yvon Horiba, France equipped with a charged-coupled device (CCD) detector and holographic notch filter.

2.2.4. Langmuir-Blodgett Film Formation System

In the preparation of monolayer and multilayers, Minimicro Langmuir-Blodgett (LB) film formation system manufactured by KSV, Finland was used. The instrument consists of a dipper motor, a PTFE trough, platinum Wilhelmy plate and 2 barriers.

2.2.5. Scanning Electron Microscope (SEM)

In the characterization of GNRs, JEOL JSM-6400 model scanning electron microscope was used.

2.2.6. Contact Angle

Attension Theta contact angle instrument was manufactured from KSV Instruments in the determination of surface modification.

2.3. Cleaning of Langmuir-Blodgett System

Before starting the experiments, calibration and cleaning procedures should be followed since even very small amount of impurities can affect the results. In order to calibrate the device, a standard weight having a known value which was measured by a calibrated balance, was used. For the cleaning procedure, first, the trough was wiped with chloroform in order to dissolve any residue on it. Then the barriers were cleaned with ethanol and rinsed with water, respectively. Finally the platinum Wilhelmy plate was washed with deionized water, acetone and chloroform. Acetone was used as an intermediate solvent.

2.4. Isotherm Experiments

Very dilute solutions were prepared and as a spreading solvent, mostly chloroform was used due to its immiscibility of water. Before starting any experiment, after the opening the barriers until the zero position which corresponds to the maximum trough area, the subphase was filled onto the trough until the level equals or is just a little bit higher than the trough edge level to prevent any leakage over the edges. Wilhelmy plate was partially immersed into the subphase. Then, both the balance value and barrier position were zeroed and the cleaning of the subphase surface was checked until the surface pressure stayed below 0.2-0.3 mN/m. If the surface

pressure increases above 0.3 mN/m, then it is recommended to clean the surface of the subphase with an aspirator or a suction pipette. Specific volume of solution was spread over the subphase surface as droplets with the help of the micro syringe. For every experiment, a file was created and the parameters such as concentration, volume, subphase, compression speed and the target value for the compression were entered. We set target in terms of barrier position to achieve maximum compression within the limits of the trough dimensions. It was waited for solvent evaporation for 10 minutes before starting the monolayer formation. With a certain compression speed, initially disordered amphiphilic molecules were getting closer and ordered, phase transitions were monitored and at a specific surface pressure, the monolayer was obtained. The instant mean molecular area and surface pressure were calculated automatically by the instrument with given concentration and volume data of the solution during the experiment. Finally, the isotherm graph which was labelled surface pressure versus mean molecular area was obtained.

2.5. Surface Modifications of Glass Substrate

For the deposition experiments, glass slides (20 x 20mm having thickness 0.13-0.17mm) were used. Before using, they were modified as hydrophilic or hydrophobic depending on the desired experiment. Hydrophilic treatment was performed with based piranha solution. The solution was prepared by adding hydrogen peroxide (H_2O_2, %25) to ammonia (%25) in 1:1 volume ratio. The glass slides were waited in the solution at 60°C for 20 minutes. After that, they were washed with DI H_2O and dried with N_2 gas before using. In order to obtain hydrophobic surface, slides were modified firstly hydrophilic as described before and then, 0.2 M chlorotrimethylsilane hexane solution was prepared and slides were and waited for 2 hours in this solution. The process was summarized in Figure 2.1[42] .

Figure 2. 1 Surface modification of glass substrate (A surface of glass substrate, B hydrophilic treatment with base piranha solution, C hydrophobic treatment with chlorotrimethylsilane) [27]

2.6. Deposition of Monolayers onto a Solid Support

Cleaning procedures mentioned before were repeated for deposition experiments. Before the experiment, the modified solid substrate was attached to the dipping arm of the instrument. Depending on the transfer type, the zero line where the substrate touched the subphase surface was determined. For Y (head-to-head and tail-to-tail) or Z-type (head-to-tail and heads toward support) transfers, after determination of the zero line, substrate was immersed into the subphase at a certain level and then substance was spread over the subphase. Before deposition, the surface pressure where the solid-like monolayer obtained in the isotherms should be controlled and as a target surface pressure that previously determined value should be chosen. After the evaporation of solvent, the barriers compressed the molecules until the target surface pressure and when it was reached, the barriers tried to keep constant at that value and the transfer was started with a certain dipping rate in the upstroke direction. The substrate was completely withdrawn, the first layer deposited on it. For Y-type multilayer structure, this process was repeated both upstroke and downstroke directions with initially formed monolayer. On the other hand, to obtain

Z-type, only upstroke transfer was performed and after each transfer, the substrate was immersed into the subphase before preparing the monolayer on the surface. For X-type (head-to-tail and tails toward support) deposition, the substrate initially should be modified hydrophobic and the transfer should be performed only downstroke direction.

When the substrate reached to a certain level into the subphase, the remaining molecules should be removed from the surface and after that, the support should be withdrawn. In this particular study, only Z and Y-type multilayers were prepared.

2.7. Optimization Studies of SA Monolayers

At the beginning of the experiments considering Langmuir film formation, firstly some optimization studies were completed with the stearic acid which is the standard material of this method. Figure 2.2 represents the chemical structure of the stearic acid.

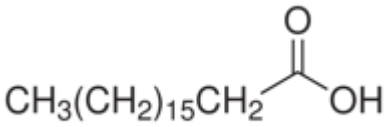

Figure 2. 2 Structure of stearic acid

Stearic acid is mostly used amphiphile for monolayer and multilayer preparation up to now. So before starting any experiment, the effect of some experimental parameters such as temperature, compression rate of the barriers and transfer rate of the obtained monolayers on the results were investigated.

2.7.1. Effect of Compression Rate of Barriers on SA Isotherm

To study the optimization of stearic acid isotherms, the parameters which can affect the results should be fixed. For this optimization study, the effect of different rates while compressing the molecules was investigated. For this aim, before each experiment, the compression rate value was changed between 2-12 mm/min. the isotherm results depending on different rates were compared. All the experiments were done at same conditions: constant temperature and on deionized water subphase.

2.7.2. Effect of Subphase Temperature on SA Isotherms

The optimization studies were continued with the temperature control. Very dilute, 1 mg/ml stearic acid chloroform solution was prepared. By circulating water, which was cooled in the ice bath with the help of a pump, in channels placed underneath the through, it was thermostated. After waiting for 15 minute in order to stabilize it, the temperature of the subphase was decreased and kept constant at 5°C. The results were compared with the data obtained at 20°C.

2.7.3. Effect of Transfer Rate of SA Monolayers on Transfer Ratio

In this study, in order to see the effect of the transfer rate on the quality of the transfers, different transfer speeds for the movable dipping arm were chosen. For this aim, after monolayer was compressed until the solid phase at a certin surface pressure, different dipping rate values were entered for each experiment and finally the transfer ratio results were collected.

2.8. Optimization Studies of Octadecae-1-thiol Monolayers

Optimization studies were continued with octadecane-1-thiol which is another standard material of Langmuir method. Effects of some experimental parameters such as temperature, volume and pH on the obtained isotherms of ODT monolayers were investigated. Figure 2.3 shows the chemical structure of ODT.

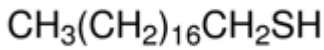

Figure 2. 3 Structure of octadecane-1-thiol

2.8.1. Effect of Subphase Temperature on ODT Isotherms

For this study, similar optimizations which were described in 2.7 were repeated for octadecane-1-thiol ($C_{18}SH$). The concentration of solution was 0.5 mg/ml, the compression rate was 8mm/min and chloroform was used as a spreading solvent and the subphase was deionized water also for these experiments. With the help of the water circulation, the ODT isotherms were obtained again at 5°C and 20°C. In order to get reproducibility of the isotherms, the experiments were repeated several times.

2.8.2. Effect of the Amount of ODT on π-A Isotherms

In this case, the effect of different volumes on the ODT isotherms was investigated. The isotherm experiments were obtained different volumes 40, 60 and 80µl. Again the concentration of solution was 0.5 mg/ml, the compression rate was 8mm/min and the temperature of the subphase was 5°C.

2.8.3. Effect of pH on ODT Isotherms

To clarify the effect of pH on ODT isotherms, the measurements were done at different pH values. Firstly, at pH 2 and secondly, at pH 10 in addition to pH 6 which was the pH value of the deionized water were studied. These two very high and very low pH values were chosen to see drastic changes and to make comparisons in the isotherms. Experiments were performed at constant temperature and constant compression rate and subphase was deionized water.

2.9. Optimization Studies of Cetyltrimethyammonium Bromide Monolayers

In this part of the study, optimization studies were performed with CTAB. The effect of concentration and subphase temperature on the stability of the monolayers were investigated. Figure 2.4 represents the chemical structure of CTAB.

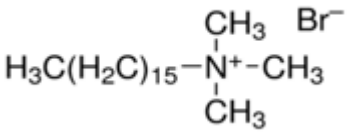

Figure 2. 4 Structure of CTAB

2.9.1. Effect of Concentration on CTAB Isotherms

The isotherm experiments were done for CTAB in this study. The first optimization study was performed with concentration. Due to its solubility in water, the concentration was a key parameter for the preparation of Langmuir monolayers with CTAB. So, to see the amount of concentration for the preparation of stable monolayers clearly, the solutions having different concentrations such as 2, 1, 0.25 and 0.15 mg/ml were prepared in chloroform solvent and the isotherm experiments were completed with these solutions at same volume and constant temperature which were 40µl and 21°C respectively. Subphase was deionized water.

2.9.2. Effect of Subphase Temperature on CTAB Isotherms

For this study, isotherms were obtained at 8, 21 and 38°C. The subphase was DI water, the volume was 100 µl, the concentration was 0.15 mg/ml and as spreading solvent, chloroform was used for all the experiments. To obtain reproducible results, experiments were repeated several times.

2.10. Gluing of CTAB Monolayers

To determine the effect of polyelectrolyte on CTAB monolayers polystyrenesulfonate (PSS) was added into the subphase as a gluing agent. Figure 2.5 shows the sture of PSS. The reason to prefer PSS was its negatively charged nature coming from the sulfonate groups and so its tendency to oppositely charged CTAB molecules. With the help of the electrostatic interaction between CTAB and PSS, it was aimed to glue the CTAB monolayer and improve the stability of the film.

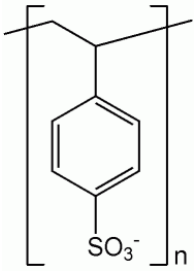

Figure 2. 5 Structure of PSS

2.10.1. Effect of PSS Concentration in the Subphase on CTAB Isotherms

In this study, the CTAB monolayers were prepared on the DI water having different PSS concentrations such as 1, 5 and 10 mM to compare the stability of the CTAB monolayers at the absence of the PSS in the subphase. All the experiments were done with same CTAB solution and same subphase temperature, 0.15 mg/ml and 21°C. All experiments were repeated many times to prove their reproducibility.

2.10.2. Hysteresis Loops of CTAB on DI Water Subphase Containing PSS

Hysteresis loops were investigated to determine the effect of the presence of PSS in subphase on the stabilization of CTAB monolayers. Continuous compression and expansion cycles were done to have an idea about the route of the molecules getting ordered and disordered. The concentration of CTAB solution was 0.15 mg/ml and the temperature was 20°C for all experiments. The hysteresis loops were also optimized changing the target option for the expansions and compressions and the waiting time after compressions and waiting position. The first part of hysteresis study was performed by waiting 4 minutes after first compression at a target surface pressure which was 35 mN/m with the concentrations of 1.0, 1 and 10 mM PSS solution subphase. In the second part, the target was changed as mean molecular area and different MMA values were chosen for each experiment depending on their particular solid phase values of the isotherms and this time, it was waited after each compression cycle 5 minute before the monolayer expanded. In the next hysteresis study, it was not waited between the cycles and the target value for compression was the target barrier position 72 mm where the barriers were very close to the Wilhelmy plate and for the expansion, it was the maximum barrier distance which was 0 mm. Finally, at the last part, the hysteresis loops were obtained until the highest point of the solid phase for compression to determine the effect only caused from the PSS

concentration in the subphase. For all hysteresis studies, to see a trend clearly, 3 compression and 3 expansion (6 cycles) were completed. To get reproducible results, the experiments were repeated several times and matching the isotherms with hysteresis lines was checked.

2.11. Gold Nanorod Monolayers

In the preparation of GNR Langmuir films, firstly GNRs were synthesized and since it is required to transport GNRs from aqueous to organic media to obtain monolayer on water surface, surface modification was performed with octadecane-1-thiol. In the following sections, all steps of GNR monolayer preparation were described in detail.

2.11.1. Synthesis of Gold Nanorods

Gold nanorods were synthesized with seed mediated method previously reported by El Sayed[43]. Firstly, seed solution was prepared by mixing 5 mL, 0.20 M CTAB solution with 5 mL, 0.0005 M $HAuCl_4$ and then 0.60 mL previously cooled into the ice bath $NaBH_4$ was added. After addition $NaBH_4$, beer-like color was observed. The seed solution was stirred for almost one hour at 25 °C. Growth solution was also prepared by mixing 5 mL, 0.20 M CTAB solution and 5 mL, 0.001 M $HAuCl_4$ with 0.004 M $AgNO_3$. And as a reducing agent, ascorbic acid was added. With the addition of ascorbic acid the solution became colorless. At the final step of the synthesis, 12 µl of seed solution was added to the growth and solution was kept 28-29°C. With continuous stirring, color change was observed.

2.11.2. Surface Modification of Gold Nanorods

The synthesized gold nanorods were caped with octadecave-1-thiol (ODT) to transfer the GNRs from aqueous media to the organic one which was required for the GNR Langmuir monolayer formation. For this aim, 1mM ODT ethanol solution was prepared and 10 mL of this solution was added to 3 mL GNR solution which was previously centrifuged at 3.500 rpm for 10 minutes twice to get rid of excess CTAB. After mixing, the solution was waited for 24 hours. Then, the solution was centrifuged at 3.500 rpm for 20 min to form the ODT-capped GNRs precipitates and to remove excess ODT. The supernatant was dried with gaseous N_2 to obtain amount information of the rods. After measurement of the amount, the precipitates were dispersed in a very little amount of chloroform depending on the desired concentration[44].

2.11.3. Preparation of Hydrophobic GNR Monolayers

After surface modification of rods, 1mg/ml dilute ODT capped GNR solution was prepared in chloroform and spread on the water surface. Compression was performed until 72mm target barrier position with 8mm/min barrier compression rate.

2.12. Characterization of PSS Glued CTAB Films by Surface Enhanced Raman Spectroscopy

The effect of the PSS on CTAB monolayers and improved strength of the attachment of these PSS glued CTAB monolayers with the GNRs were investigated by comparing the intensity of raman signals. For this aim, previously transferred CTAB layer in the absence and the presence of the PSS in the subphase were gently touched to the GNR solution for 5 min using a homemade system. Firstly, the substrate was

covered with CTAB monolayer that was formed on the DI water subphase in downstroke direction. When the substrate reached to a certain level after transfer of the monolayer, the barriers were opened until the surface pressure drops zero and to be sure that there was no remaining molecules, the surface of the subphase was cleaned with the suction pipette. Finally the substrate was withdrawn with a constant rate from the subphase and then waited for dry. After that, the support was held by the moving arm of the Langmuir Blodgett instrument with a vacuum pump and it was touched horizontally to the surface of the GNR solution for 5 min and it was dried again. For the comparison, the same procedure was followed with the substrate covered by 1 layer of CTAB obtained on the subphase having different concentrations of PSS such as 1, 5 and 10 mM. Enhancement of the signal intensity of an organic dye which is BCB (brilliant crystal blue) on the prepared substrates was compared.

CHAPTER 3

RESULTS & DISCUSSION

3.1. Optimization Studies of Langmuir Films

In order to obtain quality monolayers and the transfer of these monolayers appropriately onto a solid support directly depend on the some experimental parameters such as temperature of the subphase, compression rate of the barriers and transfer rate of the monolayer. These parameters have a great importance during both the preparation of the monolayers and the deposition of them from subphase surface onto a substrate. So, to investigate the effects of these parameters on the SA, ODT and CTAB film preparation and film deposition, they were optimized in the following study.

3.1.1. Stearic Acid Langmuir Blodgett Films

3.1.1.1. Effect of Compression Rate of Barriers on Stearic Acid π-A Isotherms

Optimization studies were started with the effect of compression rate of moving barriers on the stearic acid isotherms. Experiments were done with the different compression rates change between 2-10 mm/min. The results were shown in Figure 3.1.

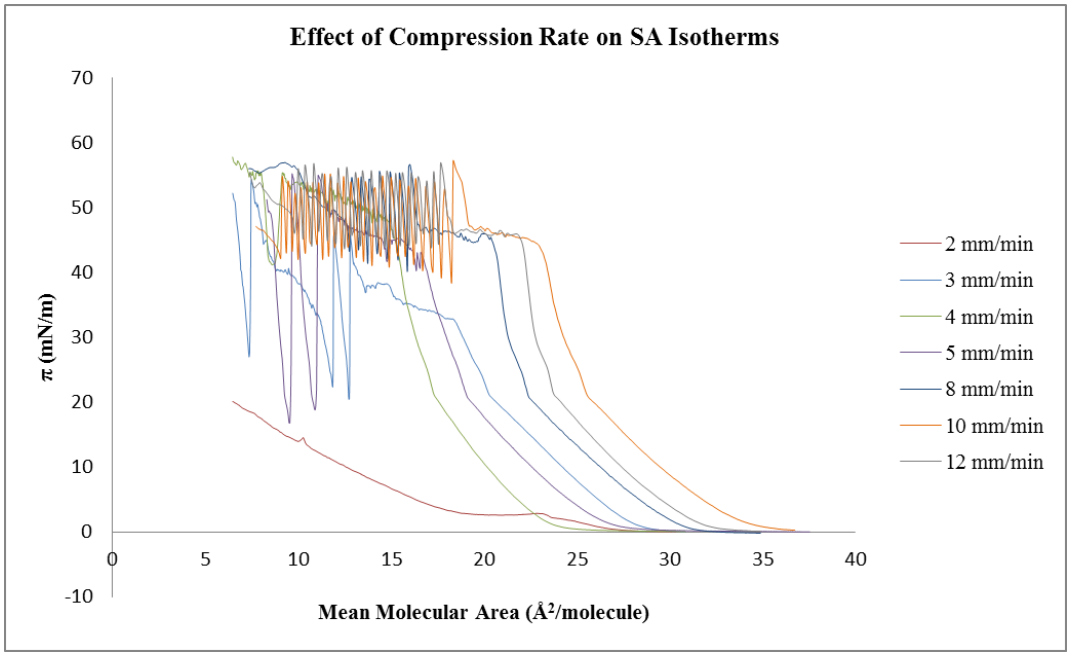

Figure 3. 1 Effect of compression rate of movable barriers on isotherms of 1 mg/ml, 20µl of SA solution in $CHCl_3$ at 5°C

As it is seen from the obtained results, the phases are less stable and highly affected from compression rates below 4 mm/min. For the 2 mm/min, especially, the monolayer could not be hold together. In order to see the effect of compression rate on the isotherms clearly, surface pressure trends after collapse points were investigated. Figure 3.2 shows the collected results.

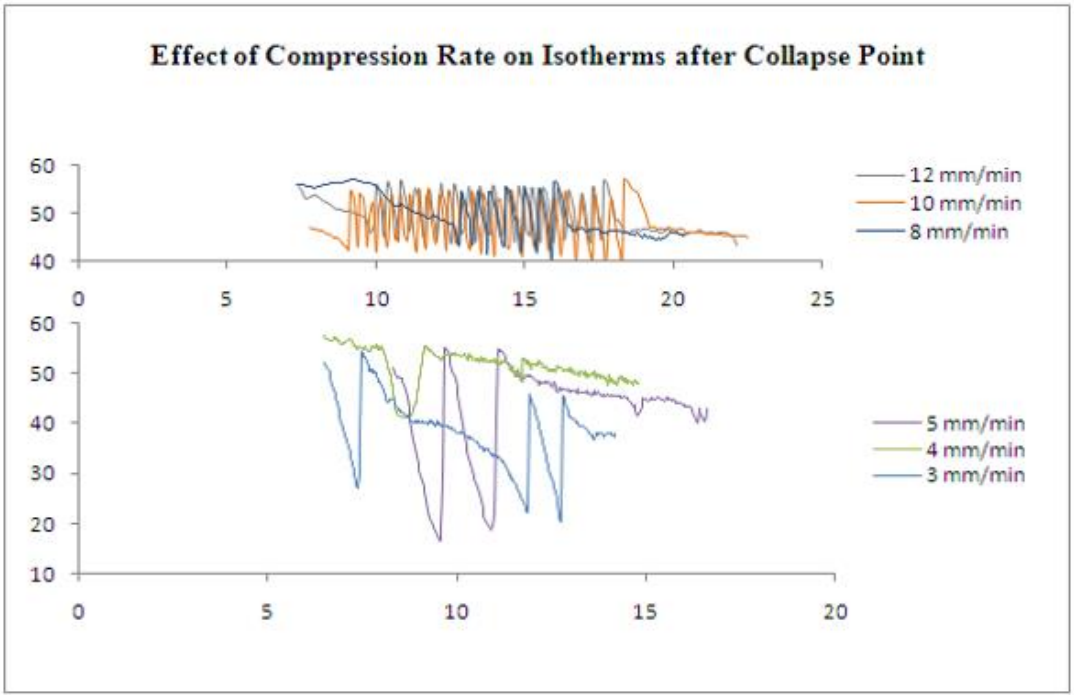

Figure 3. 2 Effect of compression rate of movable barriers on SA isotherms after collapse points of monolayers

In order to recognize the difference, data were separated in two section. The first one is consisting of 5 mm/min and lower compression rates and the second one includes 8mm/min and higher ones. In the first group, sharp increases and decreases occur in surface pressure which implies lower stabilities were obtained at lower compression rates. For the latter group, the surface pressure values changed in a smaller range which means more stabilized monolayers can be obtained by compressing the molecules at relatively higher rates. For 8 mm/min, results were highly reproducible and eventually, 8 mm/min is chosen for all other SA experiments as an appropriate compression rate.

3.1.1.2. Effect of Subphase Temperature on Stearic Acid π-A Isotherms

In order to investigate the effect of subphase temperature on stearic acid isotherm, the experiments were performed at 5℃ and 20℃. The comparison between two temperatures is shown with the Figure 3.3.

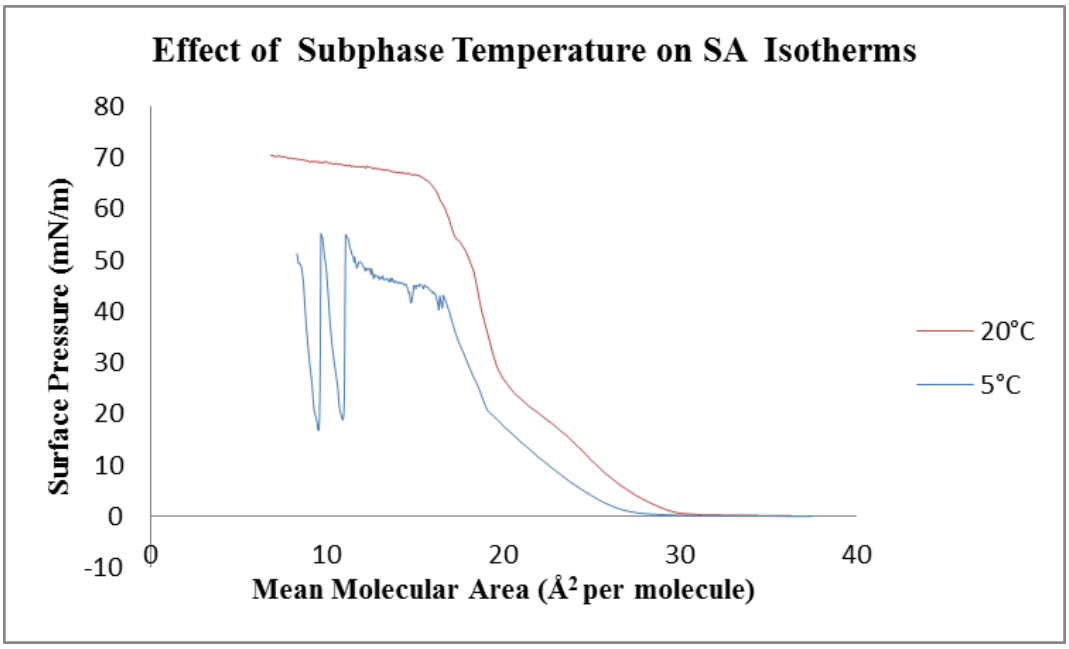

Figure 3. 3 Effect of subphase temperature on isotherms of 1 mg/ml, 20 µl SA solution in $CHCl_3$ on DI H_2O subphase

For the isotherms, distinct changes in the slopes imply that the phase transitions are existing and at both temperatures, collapse points can be observed. However at 5°C, there is a shift to the lower mean molecular areas for liquid and solid phases and at

20°C, the collapse point of the isotherm reaches to higher surface pressure. In addition to that, at 5°C there are sharp increases and decreases in the surface pressure after the collapse point. When the results are compared with the literature, they were consistent with each other. According to a study of Kato and coworkers, pressure-area (π-A) Langmuir isotherms are highly dependent on subphase temperature. The cusp point which is an indicative point for the existence of two states simultaneously shifts to higher surface pressures if the temperature of the subphase is increased. They explained this behavior with increased chain flexibility and so degree of thermal motion as the temperature increases[45]. As a result, optimization of temperature is completed and the rest of the experiments with SA were performed at 20℃.

3.1.1.3. Deposition of Stearic Acid Monolayers onto a Solid Support

Before starting the depositions, surface of the substrates were modified hydrophilic and hydrophobic depending on the type of the transfer. Hydrophilic treatment was performed with piranha solution and for the preparation of hydrophobic surface, chlorotrimethylsilane (CTMS) hexane solution was used. The contact angle data were shown in Figure 3.4.

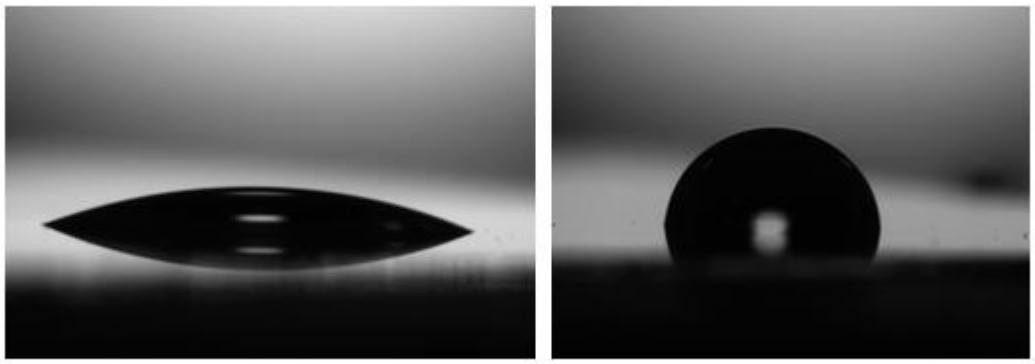

A **B**

Figure 3. 4 Contact angle images of **A** hydrophilic **B** hydrophobic surface

The contact angle was 23.9° after the piranha and 91.5° after CTMS treatment. After the fundamental optimization studies were completed for the stearic acid, the transfer of the monolayers onto a solid support were performed. Firstly Y-type multilayers were prepared and the corresponding transfer ratio results which give an idea about the quality of the transfers shown below in Table 3.1.

Table 3. 1 Transfer ratios of SA multilayers

Layer no	Direction	Total TR
1	Up	1.179
2	Down	0.086 ✗
3	Up	1.036
4	Down	0.067 ✗

Table 3. 1 (continued)

Layer no	Direction	Total TR
1	Up	1.036
2	Down	0.330 ✗
3	Up	0.960
4	Down	0.678 ✗

Layer no	Direction	Total TR
1	Up	1.115
2	Down	0.612 ✗
3	Up	0.912
4	Down	0.859 ✓

Layer no	Direction	Total TR
1	Up	1.079
2	Down	0.819 ✓
3	Up	0.919
4	Down	0.915 ✓
5	Up	0.941
6	Down	0.994 ✓
7	Up	0.925

Layer no	Direction	Total TR
1	Up	1.192
2	Down	0.120 ✓
3	Up	1.029
4	Down	1.010 ✓
5	Up	0.960
6	Down	1.073 ✓
7	Up	0.908

Transfer ratios of the early studies presented in the first three boxes. In these group of experiments, the TR values for the deposition of the even number of layers which means 2^{nd}, 4^{th}, 6^{th} layers were very low. As it was explained before, for a good transfer, transfer ratio should be close to 1. Therefore these low results mean that the depositions could not be achieved perfectly. However, further experiments prove that better results can be obtained for both even and odd number of depositions just by tuning the target surface pressure value. The target surface pressure before starting the transfer was 30mN/m for the first three experiments, whereas it was 40mN/m for the remaining experiments. This implies that when a higher target surface pressure was chosen, more rigid monolayer can be obtained which helps to improve the quality of transfer and the transfer ratio. Collected results lead to make a generalization that to make an ideal deposition, the appropriate target surface pressure where the solid-like monolayer is obtained should be determined.

After Y-type multilayers formed, Z-type multilayers were prepared and good TR results were obtained. The data shown in Table 3.2

Table 3. 2 Transfer ratios of Z-type SA monolayer and multilayers with different number of layers

i. SA 1L-Z Type

Layer no	Direction	Total TR
1	Up	1.137

ii. SA 2L-Z Type

Layer no	Direction	Total TR
1	Up	1.060
2	Up	1.156

Table 3. 2 (continued)

iii. SA 4L-Z Type

Layer no	Direction	Total TR
1	Up	1.233
2	Up	1.019
3	Up	1.161
4	Up	1.152

iv. SA 5L-Z Type

Layer no	Direction	Total TR
1	Up	1.128
2	Up	1.164
3	Up	1.137
4	Up	1.085
5	Up	1.093

For Z-type multilayers, it was aimed to see the strength of the interaction between the tail and the head groups of SA by monitoring the TR results. It can be said that, all the transfers were performed perfectly since almost all the TR values were very close to 1 which means the interaction between the acidic head group and the chain of the SA is strong enough to obtain stabilized multilayers. So it can be concluded that, although the Y-type transfer is more practical, to build stearic acid multilayers, both Y and Z-types transfers can be used to get good quality multilayers in the deposition experiments.

3.1.1.4. Effect of Transfer Rate on Transfer Ratio of SA LB Films

To investigate the effect of transfer rate on the transfer ratio, the speed of the dipping arm were changed for each deposition and the transfer ratio results were represented in Figure 3.5.

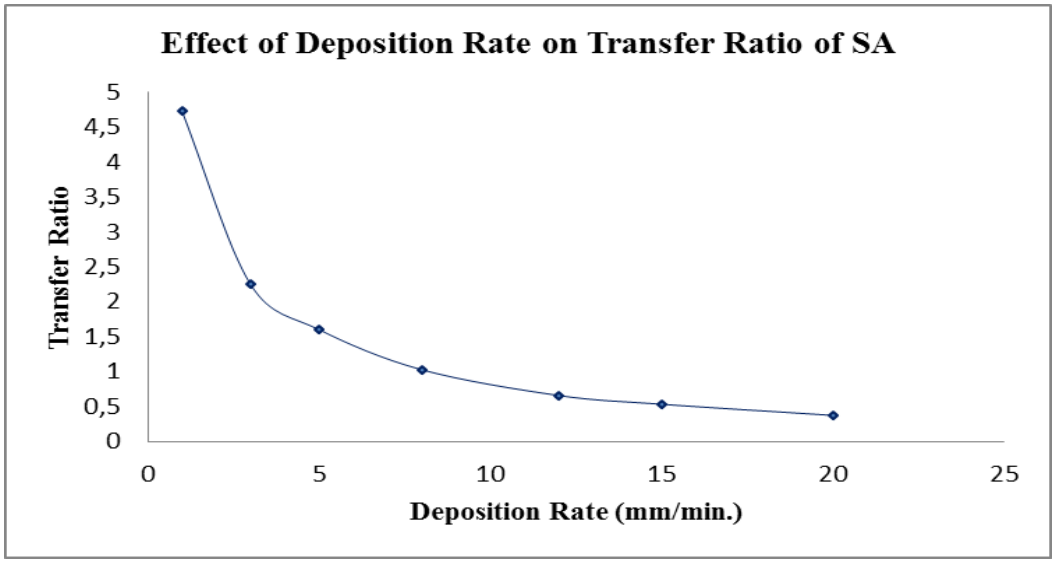

Figure 3. 5 Effect of deposition rate of dipping arm on transfer ratio of SA monolayers

Main factors that affect the stability of the transfer are the phase of the monolayer being deposited and the properties of it. The efficiency of a transfer depends on the interactions between the monolayer and the substrate surface associated with morphology and the deposition rate. Changing the deposition rate directly related with the contact angle of the substrate during the withdrawal of it from the subphase surface.

In order to do ideal depositions, this contact angle (or zipper angles) should be large since fast drift of water (subphase) from surface does not let the monolayer be

stabilized. So for the fast depositions the interaction between the substance and the substrate surface should be really strong[46].

Collected results imply that, slow transfers cause higher TR values while lower TR values were obtained at rapid depositions. As a result, to achieve ideal transfers, the transfer rate of the dipping arm should be optimized. For the SA, the optimum deposition rate was determined as 8.0 mm/min.

3.1.2. Octadecane-1-thiol Langmuir Films

π-A isotherms for Octadecane-1-thiol Langmuir monolayer is shown in Figure 3.6. Isotherms are reproducible but their shape are different from that of SA. Since thiols are less polar than carboxylic acids, distinct phase transitions could not be observed in their isotherms.

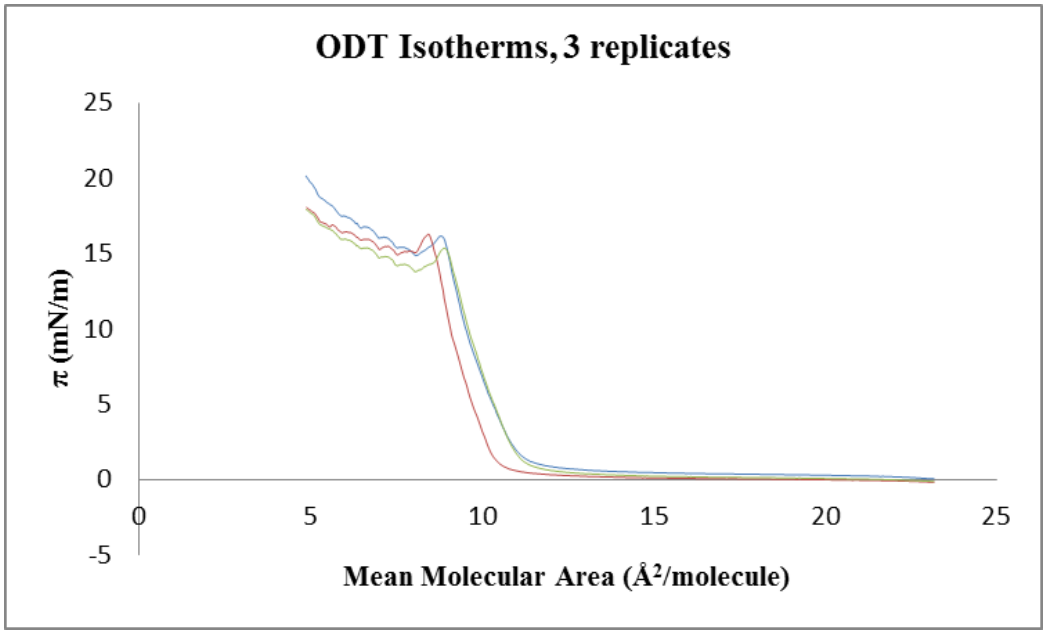

Figure 3. 6 π-A isotherms of 0.5 mg/ml, 60 µl ODT solution in $CHCl_3$ on DI H_2O subphase at 5°C, 3 replicates

As it was mentioned in section 3.1, experimental parameters are really effective in the preparation of good quality monolayers and multilayers. In this study, again effects of some parameters such as temperature of subphase, volume of spreading solution and subphase pH on ODT monolayers were investigated. Collected results were represented in the following sections.

3.1.2.1. Effect of Subphase Temperature on ODT π-A Isotherms

Firstly, the temperature optimization was done for octadecane-1-thiol at two different temperatures 20℃ and 5℃. Results were illustrated in Figure 3.7.

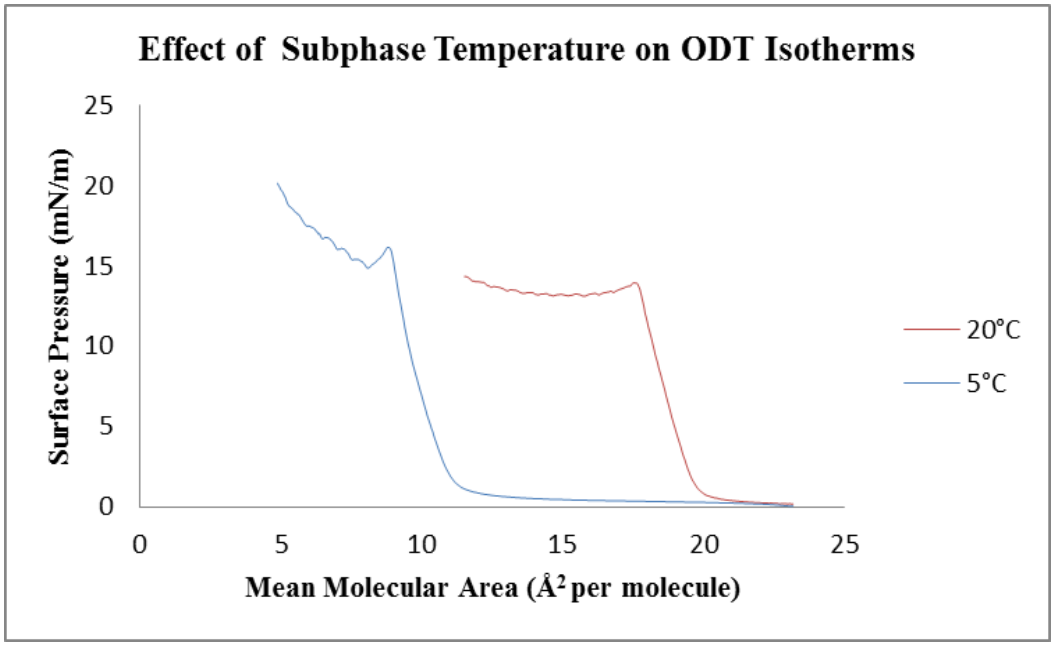

Figure 3. 7 Effect of subphase temperature on isotherms of 0.5 mg/ml, 60 µl ODT solution in $CHCl_3$ on DI H_2O subphase

Results were consistent with the previous explanations about the effect of subphase temperature on the π-A isotherms. At lower subphase temperature, a shift to lower mean molecular areas was again obtained.

3.1.2.2. Effect of the Amount of ODT on π-A Isotherms

To see the effect of the amount of ODT introduced, on the π-A isotherms, the experiments were performed at various (40, 60 and 80 µl) volumes of 0.5mg/ml ODT solution. Other parameters such as temperature and the compression rate of barriers were kept constant. The results were represented below in Figure 3.8.

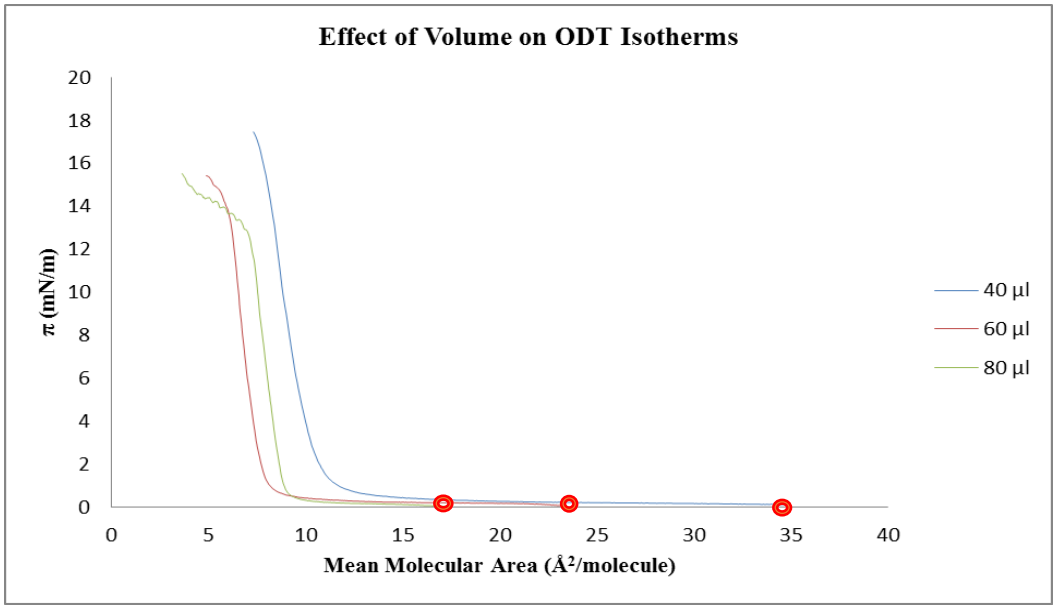

Figure 3. 8 Effect of volume of 0.5 mg/ml ODT solution in $CHCl_3$ at 20°C on DI H_2O subphase on π-A isotherms of ODT

As expected, the main difference was the starting point of the isotherms. The difference between the volumes loaded on the surface for the same concentration resulted in the different mean molecular area values. For the lower volumes, the area occupied per molecule was increased which means there are lower number of molecules on the subphase surface.

3.1.2.3. Effect of pH on ODT π-A Isotherms

The isotherms were monitored at different pH values, at pH 2, 6 and 10. The remaining parameters were constant in each experiment. Obtained data were shown in Figure 3.9.

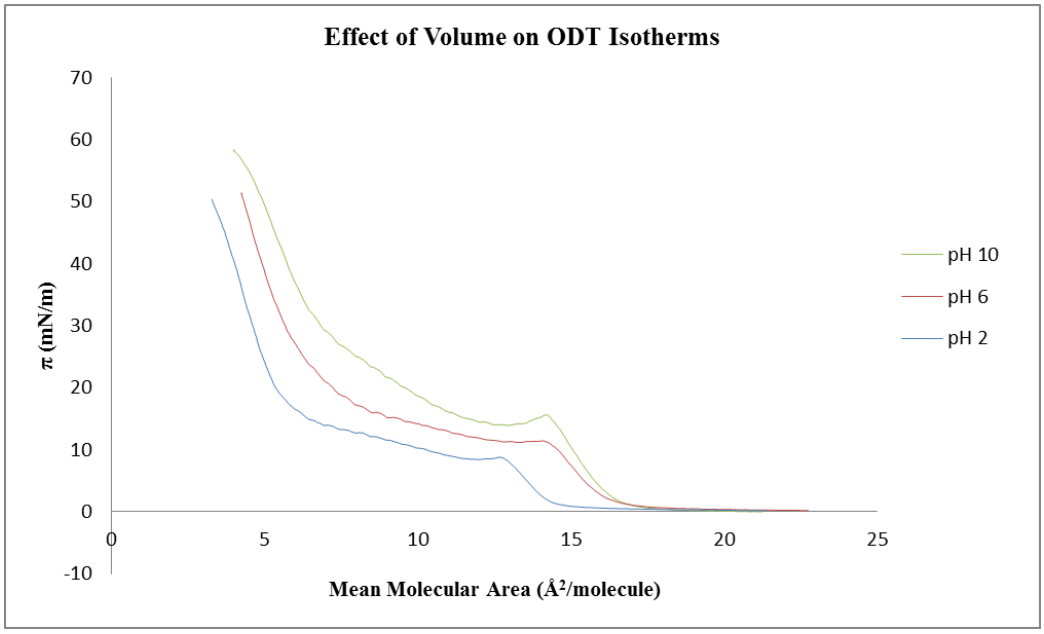

Figure 3. 9 Effect of pH of subphase on π-A isotherms of 0.5 mg/ml, 65 µl ODT solution in $CHCl_3$ at air-water interface

According to the obtained data, it can be said that; there is a shift to the lower mean molecular areas at pH 2, where gas-liquid phase transition starts approximately at 13 $Å^2$/molecule. At pH 6 and pH 10, on the other hand, the transition starts approximately at 17 $Å^2$/molecule. In addition to that, the collapse point of the isotherms reaches higher surface pressure value as the pH increases and at pH 10, the

collapse point is more distinctive compared with others. When the results were compared, they were consistent with the literature. According to the publication, namely `Langmuir-Blodgett films of octadecanethiol-properties and potential applications`, when the concentration of NaOH was increased, the isotherms shifted to the higher mean molecular areas as we observed. They explained this behavior with the dissociation tendency of weakly acidic thiol groups at basic conditions. They proved their theory with the AFM and BAM results of the monolayers[47]. Another explanation was the oxidation reaction of ODT to form dioctadecyl disulfide on the subphase surface in the presence of excess OH^- which catalysis the reaction[33]

3.1.3. Cetyltrimethylammonium Bromide Langmuir Films

In this part of the study, experiments were continued with CTAB. Since CTAB is the stabilizing agent of the GNRs in a bilayer form and our further aim was to organize and transfer GNRs in a film structure, it was required to learn the behavior of CTAB itself before doing experiments with GNRs. Therefore some experimental parameters such as concentration of spreading solution, temperature of subphase, and effect of polyelectrolyte were optimized.

As it was mentioned before, monolayers with water soluble materials such as anionic or cationic surfactants can be prepared at the air-water interface and transferred onto a substrate surface with Langmuir and Langmuir Blodgett methods. However, it was emphasized that, in order to obtain stable films with these ionic amphiphiles, they should interact with another material (i.e. stearic acid) to form a complex that acts as Langmuir compatible molecule[16,17,48–52]. Otherwise the molecules sink into the bulk phase and they do not form a monolayer at the surface. Although CTAB is a cationic surfactant, due to its high surface activity, CTAB prefers to reside on the surface[53] of the subphase. Therefore we decided to examine the properties of Langmuir film of CTAB was used without using any other material.

Although it was emphasized the requirement of the interaction of water soluble surfactants with water insoluble ones, in this study, the preparation of stable CTAB monolayers was achieved without using a complex formation.

3.1.3.1. Effect of Concentration on CTAB π-A Isotherms

The π-A isotherms for CTAB solutions were obtained using 2, 1, 0.25 and 0.15 mg/ml CTAB solutions while keeping the volume of the CTAB solution and the temperature of the subphase constant. The obtained results are represented in Figure 3.10.

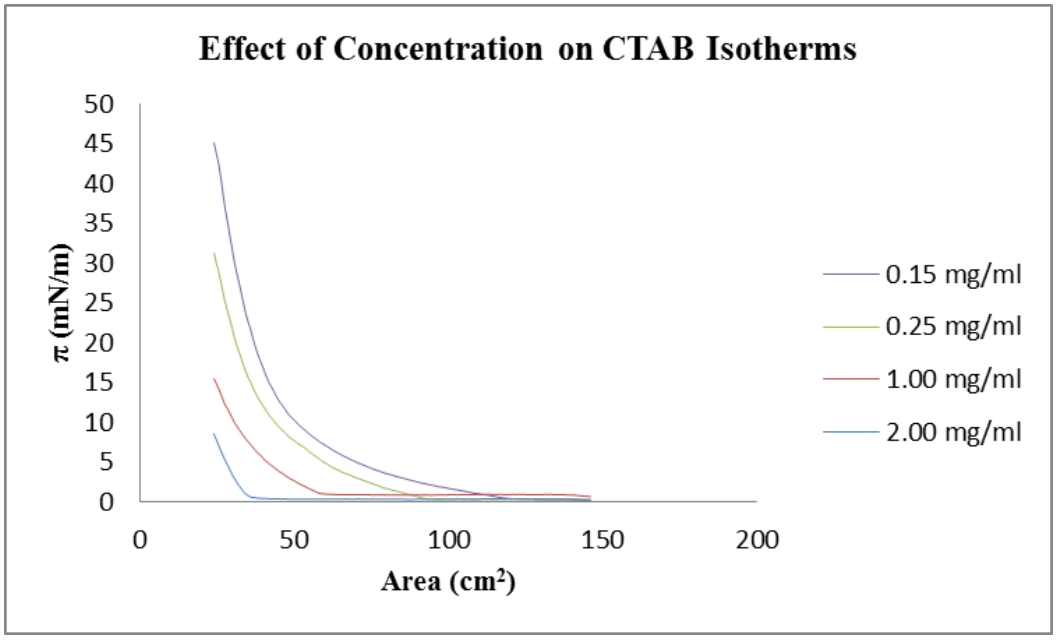

Figure 3. 10 π-A isotherms of 40µl CTAB on DI H2O subphase, 0.15, 0.25, 1.00 and 2.00 mg/ml CTAB solution in $CHCl_3$ at 20°C

According to the results, as the concentration decreases better isotherms were obtained. For the most diluted solution, a phase transition having the highest solid phase surface pressure among them was obtained. Due to its water solubility, the critical micelle concentration (cmc) of CTAB has a great importance on the π-A isotherms. The critical micelle concentration is defined as the concentration of surfactants above which micelles form and all additional surfactants added to the system go to micelles. CMC value is 0.34 - 0.36mg/ml for CTAB[54]. The effect of concentration on the isotherms directly depends on cmc. As can be seen from Figure 3.10, the solutions having 0.15 and 0.25mg/ml CTAB concentration that is below the cmc provide better π-A isotherms.

3.1.3.2. Effect of Subphase Temperature on CTAB π-A Isotherms

For this study, isotherms were obtained at 8, 21 and 38°C. To obtain reproducible results, experiments were repeated several times. Results are shown below:

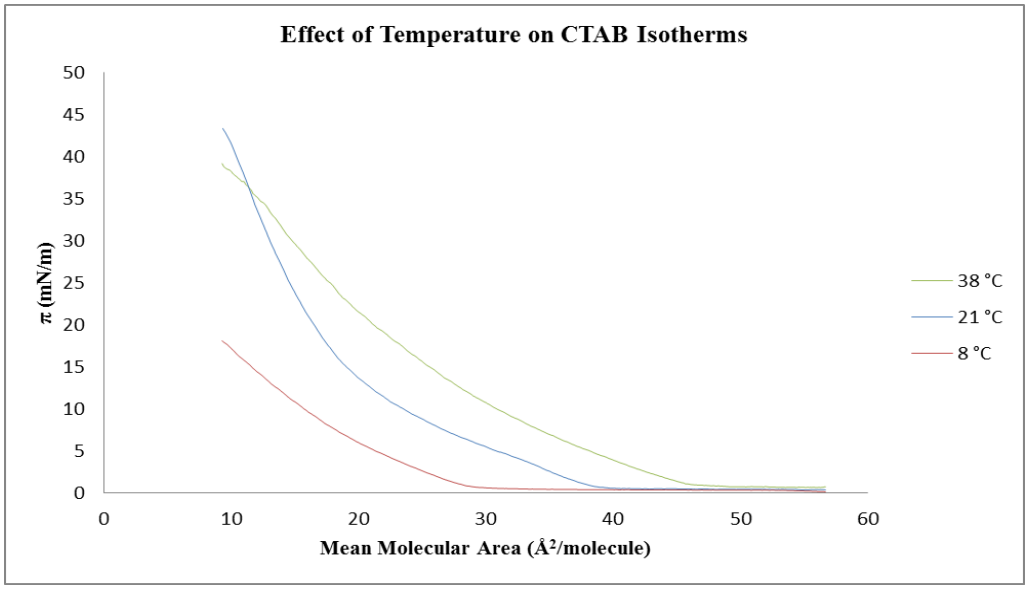

Figure 3. 11 π-A isotherms of 100µl CTAB on DI H_2O subphase, 0.15mg/ml CTAB solution in $CHCl_3$ at 8, 21 and 38°C

Figure 3.11 shows that at room temperature (21℃), the phase transitions can be distinguished clearly and isotherm reaches to the highest surface pressure value compared with the isotherms obtained at 8 and 38℃ subphase temperature. Consistent with the previous explanations as temperature increases, the isotherms shifted to the higher mean molecular areas.

3.2. Gluing of CTAB Monolayers

The first examples of 'Glued Langmuir-Blodgett Films' are introduced by Steven Regen. He used 'gluing' term for the crosslinking of layers that are prepared by charged surfactants with oppositely charged water soluble polyelectrolytes[25,26,28–30,55,56]. Regen and coworkers added the gluing material into subphase and they

recognized that, gluing provides a fundamental route for the modification of the monolayers because after gluing the organization of surfactant molecules was retained[56]. Regarding to this stability in organization, Regen achieved to increase the efficiency of the transfers of monolayers by gluing. He used long carbon chain (16 carbon) attached calixarene molecules as surfactant and suggested that, without gluing, the transferred monolayer from the surface onto a substrate at a down stroke cycle, can be return to surface again when the substrate is withdrawn. On the other hand, with the help of the ionic crosslinking between monolayer and the gluing agent, the cohesiveness of the molecules within the monolayer can be increased and so the return of the deposited monolayer onto the subphase surface can be prevented[28]. Figure 3.12 represents the effect of gluing on the efficiency of the monolayer deposition.

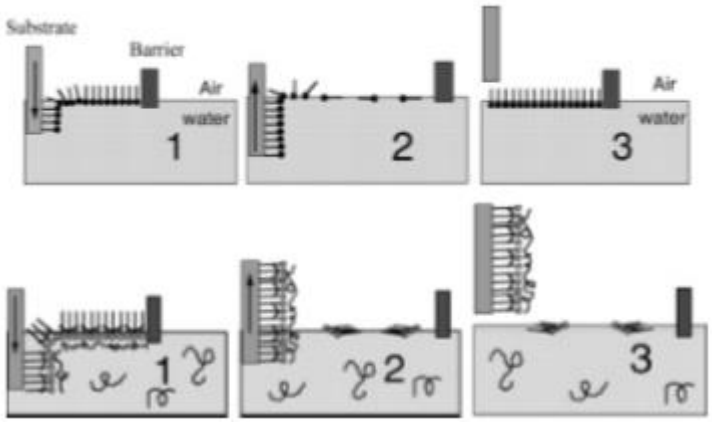

Figure 3. 12 Illustration of efficiency in the transfer of monolayer in the absence and presence of gluing[29]

We decide to apply gluing process to our LB system for the construction of CTAB monolayers. In the following study section, the effect of PSS, a counter ion polyelectrolyte, on the π-A isotherm of CTAB monolayers and their transfer onto substrate was represented.

3.2.1. Effect of PSS Concentration in the Subphase on CTAB Isotherms

In this study, the CTAB monolayers were prepared on aqueous solution of PSS having various concentrations to compare the stability of the CTAB monolayers with the one obtained on the DI H_2O subphase. All the experiments were done at the same subphase temperature and repeated several times to prove their reproducibility. Obtained data are represented in Figure 3.13.

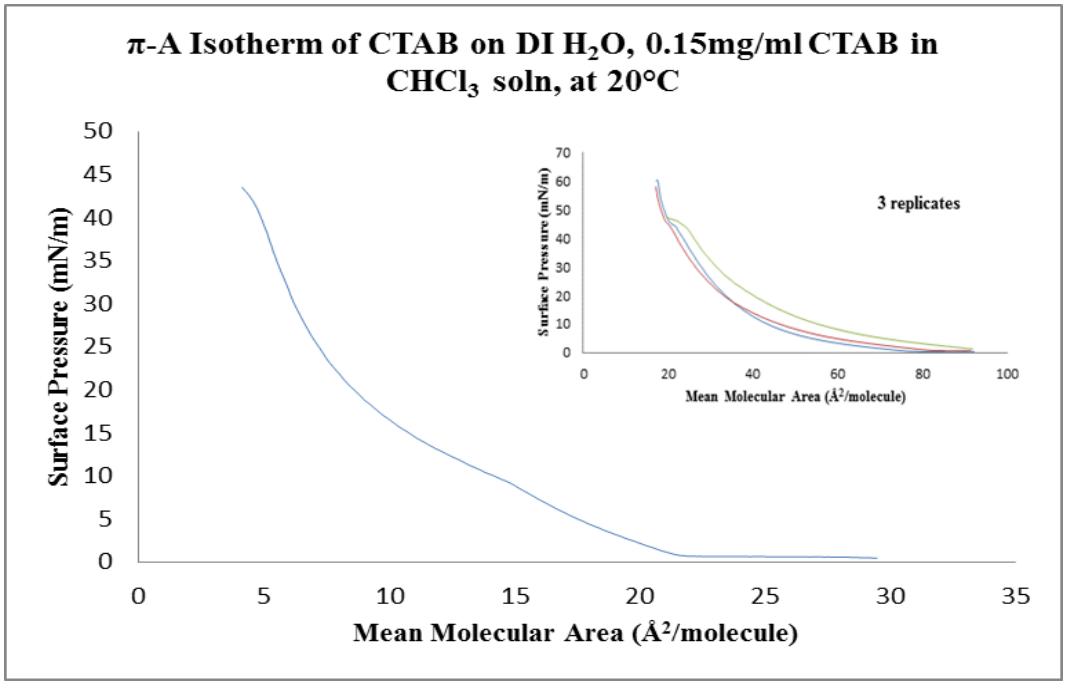

Figure 3. 13 π-A isotherm of CTAB on DI H_2O subphase, 0.15mg/ml CTAB solution in $CHCl_3$ at 20°C (inset 3 replicates)

In the π-A isotherm of CTAB obtained on DI H_2O, the phase transitions can be seen clearly with the changes in the slope of the curve. The collapse point cannot be distinguished but there exists a collapse point like break at 45 mN/m. therefore collapse point was assigned to 45mN/m. Inset figure shows that of the CTAB π-A isotherms on DI H_2O can be obtained in a reproducible manner.

Figure 3.14 represents the π-A isotherm of CTAB formed on 1mM PSS solution subphase.

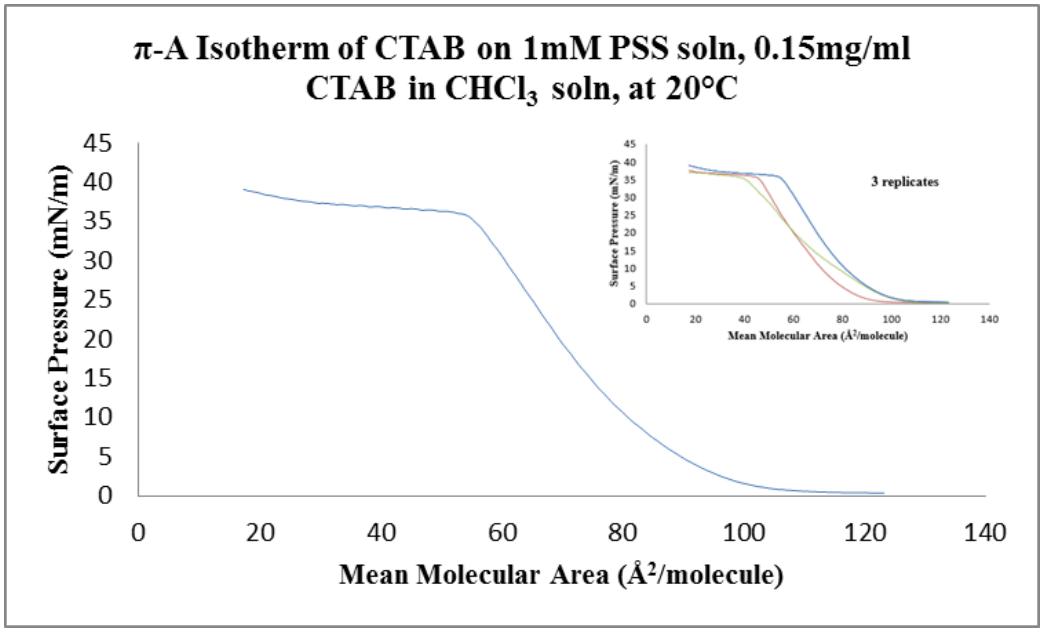

Figure 3. 14 π-A isotherm of CTAB on 1mM PSS solution subphase, 0.15mg/ml CTAB solution in $CHCl_3$ at 20°C (inset 3 replicates)

Compared with the previous experiment, when PSS was added into the subphase, the isotherm behaves differently. The surface pressure at collapse point is lower but it was more stable after collapse point. The phase transitions can be obtained clearly and the collapse point is more significant. Again the experiments were performed repeatedly and the inset figure implies that the π-A isotherms of CTAB on 1mM PSS solution subphase were consistant with each other.

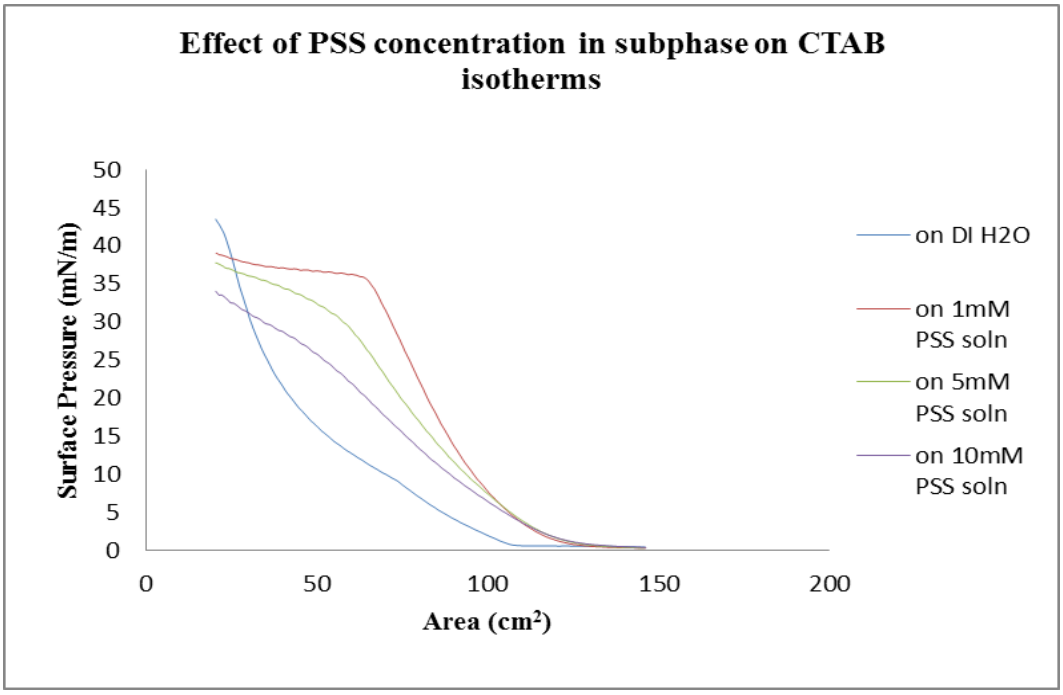

Figure 3. 15 Effect of PSS concentration on CTAB isotherms, 0.15mg/ml CTAB solution in $CHCl_3$ at 20°C

Figure 3.15 exhibits the effect of PSS amount in the subphase on CTAB isotherms. The main reason to prefer PSS was its negatively charged nature coming from the sulfonate groups and so its tendency to oppositely charged CTAB molecules. With the increase in the amount of the PSS in the subphase, the distinctive phase transitions and collapse points started to dissappear slightly with decrease in the collapse point surface pressures. When the isotherms were compared at the absence and the presence of the PSS, it was recognized that, the phase transitions started earlier.

Regen and coworkers explain the dependency of the PSS concentration in subphase for the calixarene bilayers by investigating the viscosity of the surface, TR results of the monolayers and selectivity in permeation. They concluded that the extent of the

crosslinking directly depends on the amount of PSS. According to their model, the increase in the PSS amount means much more polymer chains which compete for the ionic parts of the monolayer. If the concentration of PSS decreases, the crosslinking increases with less competition[25].

In order to see the effect of PSS in the subphase on the CTAB monolayers clearly, the hysteresis experiments were performed in the following study.

3.2.2. Hysteresis Loops of CTAB on PSS Solution Subphase

Hysteresis curves generally give an information about the stability of the monolayers with the repeated compression and expansion cycles by looking the behavior of the molecules or the path they followed during the process. When the molecules are initially compressed, molecules start to come together with the force applied by the moving barriers and the phase transitions are observed. If the monolayer is expanded after the compression, there may occur two different behaviors. In one of them, the molecules may start to go far from each other in the same way how they compressed or they may expand in a different route. The former state implies that the molecules are getting together by just the effect of barriers and when they form monolayer, they do not have any tendency to stay together and so with the removal of the force applied by barriers, they move away in the same way and it is monitored as a two matching or very close curves from the instrument. However in the later one, if there is an interaction between the molecules, it leads to molecules stay together and when they are expanded, another isotherm different from the compression curve is obtained. That means the molecules do have hysteresis[57]. Alternatively, the hysteresis loops may stabilize with the increasing number of compression-expansion cycles. For this behavior of molecules, there is another explanation in the literature. In one of their studies, Ahmad and coworkers investigated the hysteresis behavior of octadecanoic acid, octadecylamine and octadecanethiol using different plates such as platinum, glass and paper. The reason for using different plates is to see the effect of

contact angle on the hysteresis curves during the experiments. They concluded that while the contact angle for octadecylamine increases in platinum and glass ones, for octadecanoic acid and octadecanethiol, it slightly changed due to the adsorption on platinum and also glass is relatively low. It implies that contact angle for octadecanoic acid and octadecanethiol remains constant during all the cycles[58]. The study shows that, the change in just the 1st compression-expansion cycle and different from the remaining matched loops can be caused by the change in the contact angle during the 1st cycle.

With the help of these findings, in the following study, hysteresis loops were investigated to determine the effect of PSS in subphase on the stabilization of CTAB monolayers. The concentration of CTAB solution was 0.15 mg/ml and the temperature was 20°C for all experiments. The first part of hysteresis study was performed by waiting 4 minutes only after the first compression at a target surface pressure which was 35 mN/m. It was aimed to see the effect of PSS on CTAB isotherms waiting for a while after first compression which may help to increase the stability of the monolayer. Results were shown following figures.

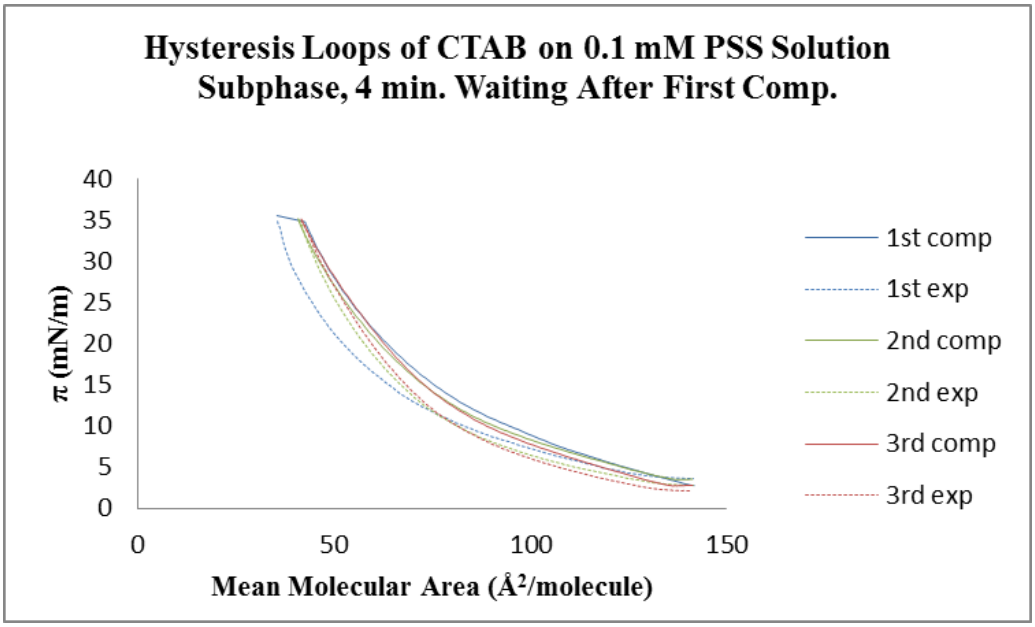

Figure 3. 16 Hysteresis loops of CTAB on 0.1mM PSS solution subphase, 0.15mg/ml CTAB solution in $CHCl_3$ at 20°C, it was waited for 4 min after 1st compression at target surface pressure 35 mN/m

Figure 3.16 shows the hysteresis loops of CTAB obtained on 0.1mM PSS solution subphase. It can be said that with the effect of the waiting at the end of the first compression cycle, the first expansion shifted to lower mean molecular areas. However after the first cycle, monolayer compressed and expanded almost same way.

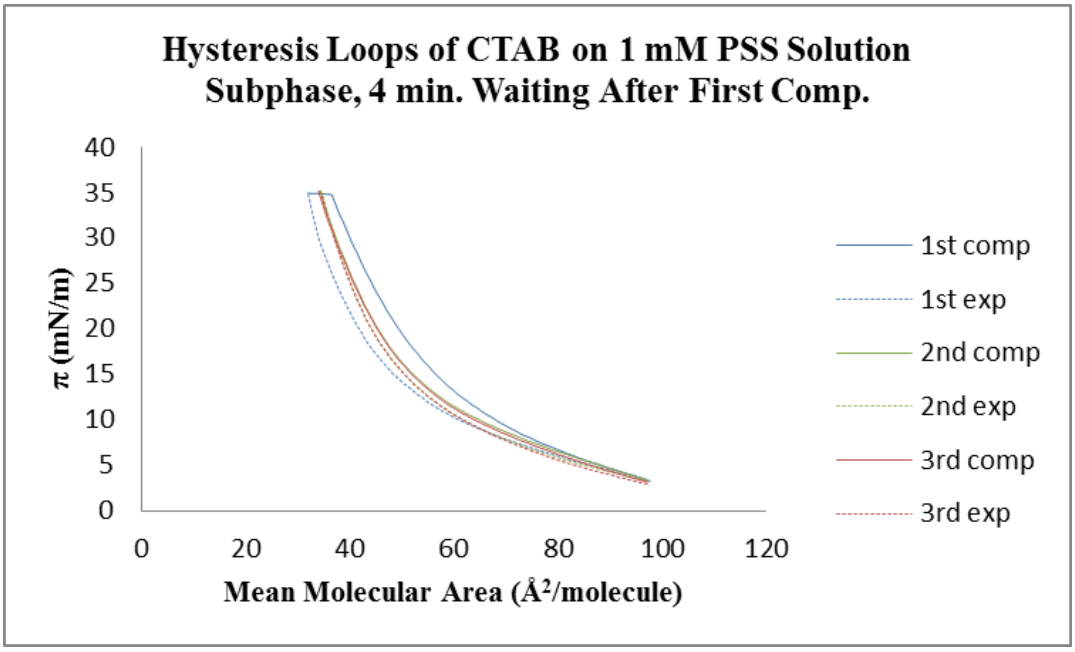

Figure 3. 17 Hysteresis loops of CTAB on 1mM PSS solution subphase, 0.15mg/ml CTAB solution in $CHCl_3$ at 20°C, it was waited for 4 min after 1st compression at target surface pressure 35 mN/m

Hysteresis loops of CTAB on 1mM PSS solution subphase was represented in Figure 3.17. In this time, the shift was lower compared with the previous one and after the first compression-expansion loop was completed, the cycles were stabilized.

Hysteresis loops of CTAB on 10mM PSS solution subphase was shown in Figure 3.18.

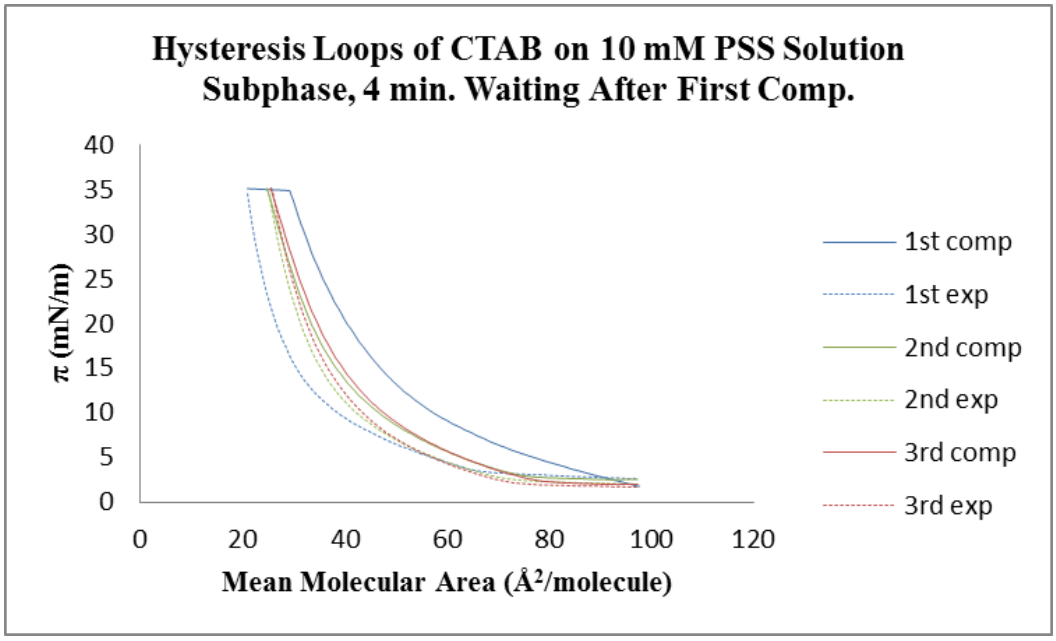

Figure 3. 18 Hysteresis loops of CTAB on 10mM PSS solution subphase, 0.15mg/ml CTAB solution in $CHCl_3$ at 20°C, it was waited for 4 min after 1st compression at target surface pressure 35 mN/m

According to data, it was obvious that, the largest shift was obtained when the hysteresis was performed on 10mM PSS solution. Again, mostly stabilized loops were obtained for remaining cycles.

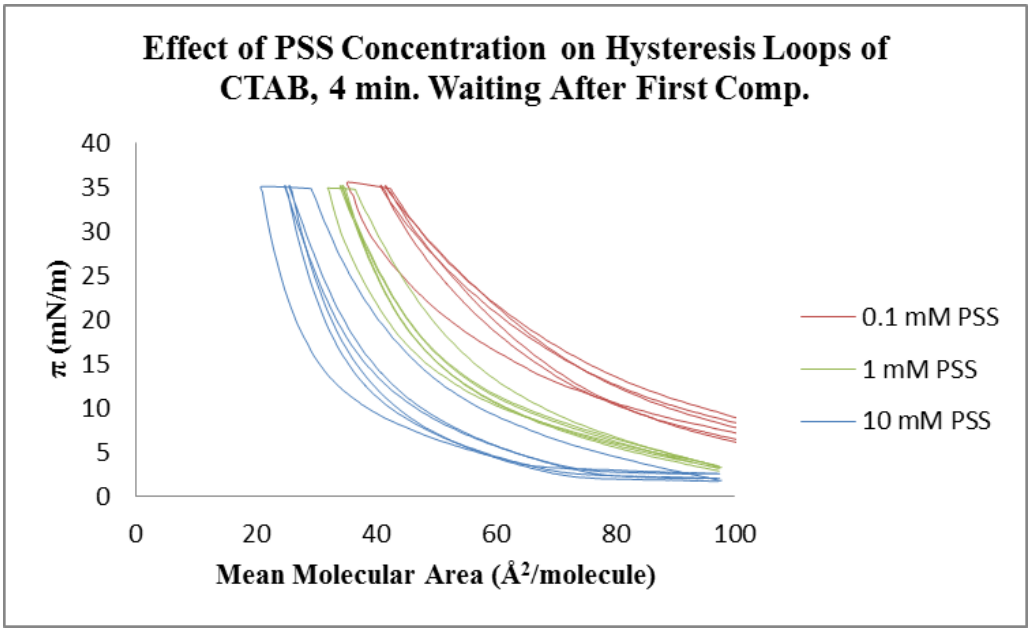

Figure 3. 19 Effect of PSS concentration in subphase on hysteresis loops of CTAB, it was waited for 4 min after 1st compression at target surface pressure 35 mN/m

In order to see the effect of PSS amount on the hysteresis loops of CTAB, obtained results were illustrated in the same figure. Figure 3.19 implies that for the first expansions, a shift to the lower mean molecular areas was observed but further loops were matching each other. There was no trend such an increasing PSS concentration causes lager shifts. For the isotherm obtained on 0.1mM PSS caused larger shift than 1mM. Regen was also recognized the same situation in his studies. He observed that the TR values for the transfer of calixarene monolayers from the subphase containing 0.1mM PSS were not close to 1 while ideal depositions were performed for the other concentrations. They suggest that 0.1mM PSS causes high crosslinking that prevents the effective deposition[25].

In the second part, the target was changed as mean molecular area and different MMA values were chosen for each experiment depending on their particular solid phase values of the isotherms and this time, it was waited after each compression cycle before the monolayer expanded. Figure 3.20 shows the hysteresis loops obtained at the absence of PSS in the subphase.

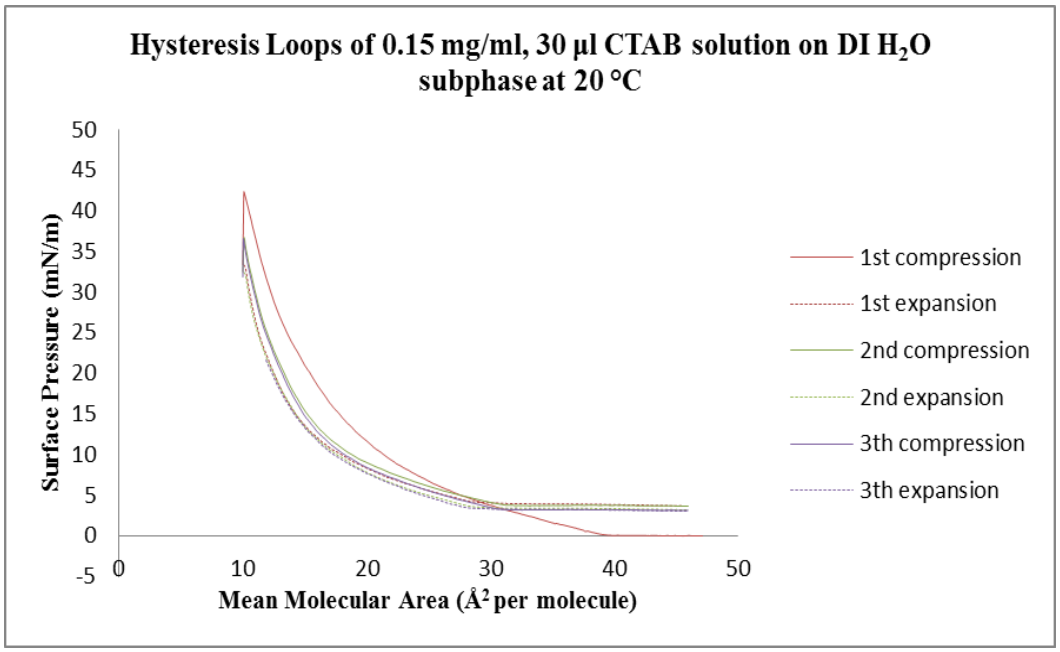

Figure 3. 20 Hysteresis loops of CTAB on DI H2O subphase, 0.15mg/ml CTAB solution in $CHCl_3$ at 20°C, it was waited for 5 min after 1st compression at target mean molecular area 10 $Å^2$/molecule (return target 46 $Å^2$/molecule)

It can be said that except from the first compression, all other loops were almost parallel to each other.

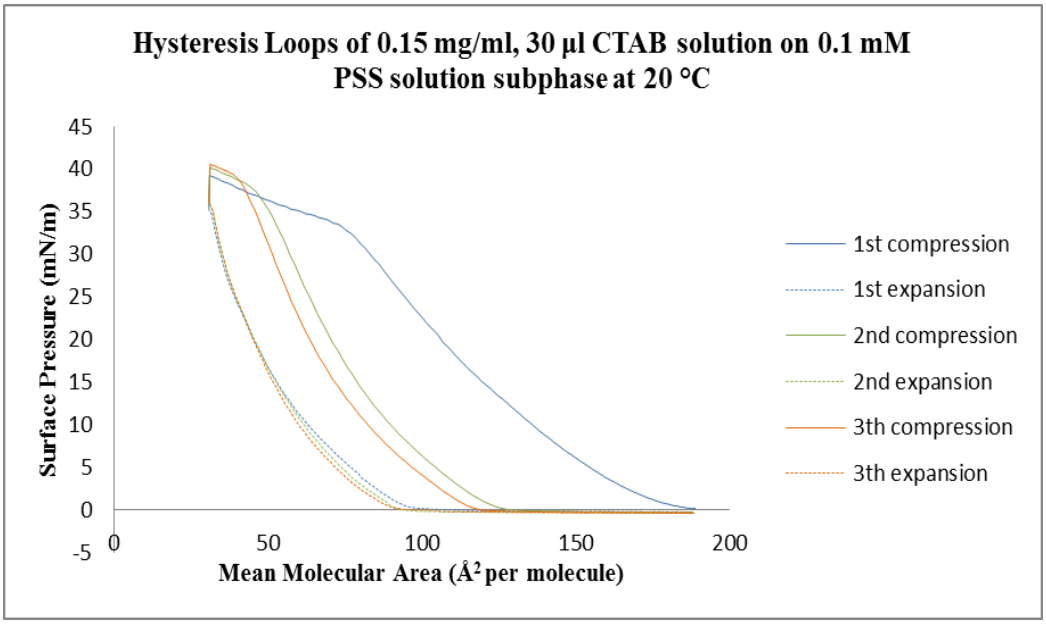

Figure 3. 21 Hysteresis loops of CTAB on 0.1mM PSS solution subphase, 0.15mg/ml CTAB solution in $CHCl_3$ at 20°C, it was waited for 5 min after 1st compression at target mean molecular area 10 $Å^2$/molecule (return target 46 $Å^2$/molecule)

Figure 3.21 represents the hysteresis loops for the CTAB monolayer on 0.1 mM PSS solution subphase. The main diffrence was the significant shift to the lower MMA for all compressions while all expansions were matched. Hysteresis loops of CTAB on 1mM PSS solution subphase is illustrated in Figure 3.22.

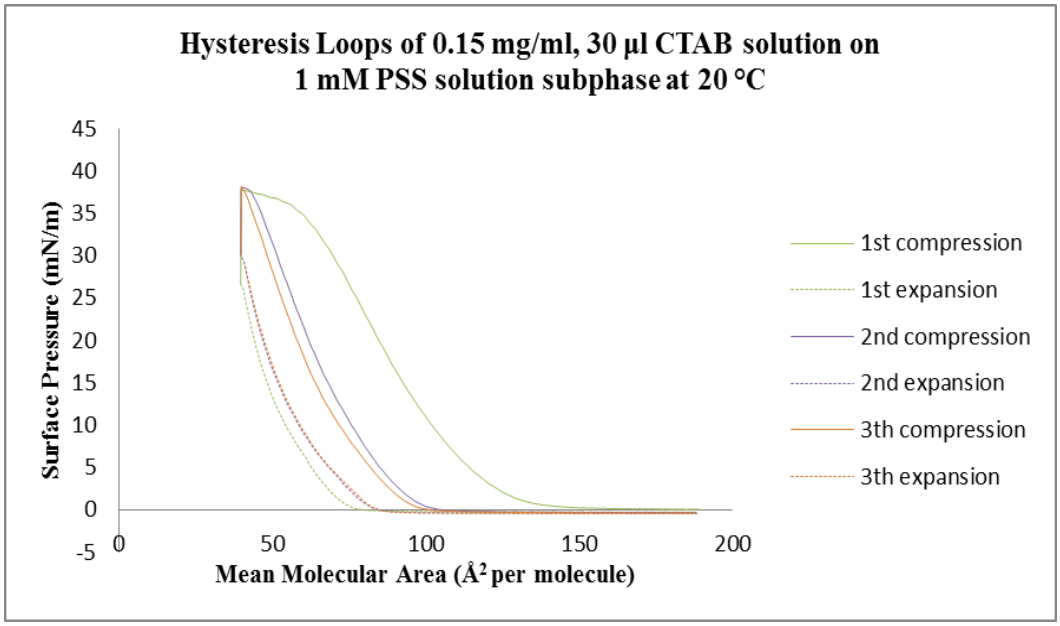

Figure 3. 22 Hysteresis loops of CTAB on 1mM PSS solution subphase, 0.15mg/ml CTAB solution in $CHCl_3$ at 20°C, it was waited for 5 min after 1st compression at target mean molecular area 10 $Å^2$/molecule (return target 46 $Å^2$/molecule)

The compressions were again shifted to the lower MMA as the number of cycles increases. The drop in the surface pressure was higher compared with the previous one.

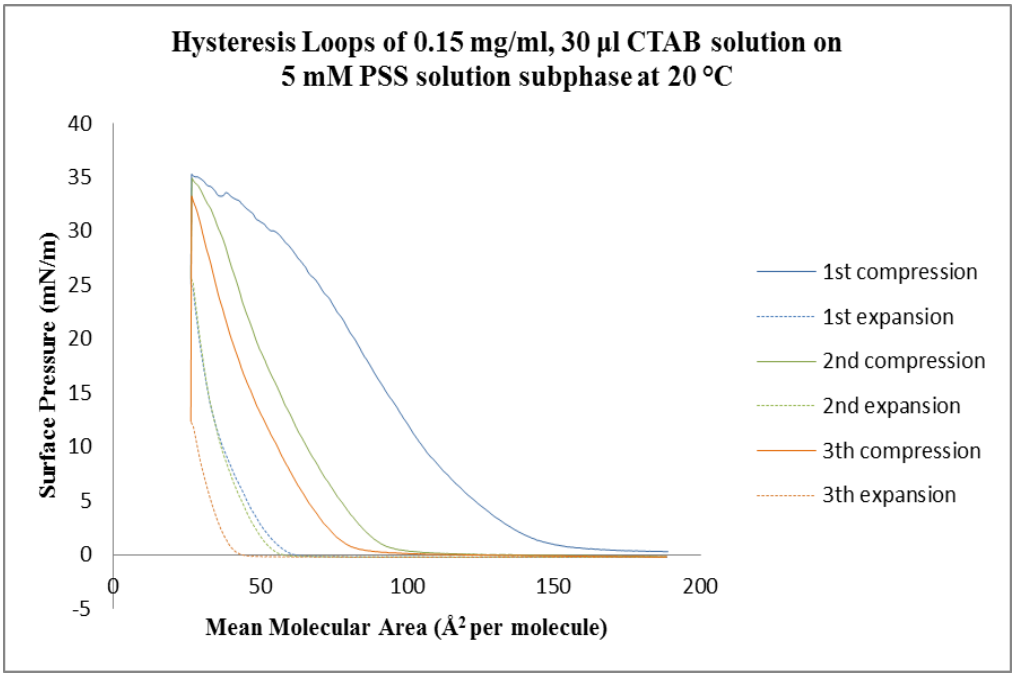

Figure 3. 23 Hysteresis loops of CTAB on 5mM PSS solution subphase, 0.15mg/ml CTAB solution in $CHCl_3$ at 20°C, it was waited for 5 min after 1st compression at target mean molecular area 10 $Å^2$/molecule (return target 46 $Å^2$/molecule)

Hysteresis loops of CTAB on 5mM PSS solution subphase was illustrated in Figure 3.23. The shift and also the decrease in the surface pressure were more significant in this experiment.

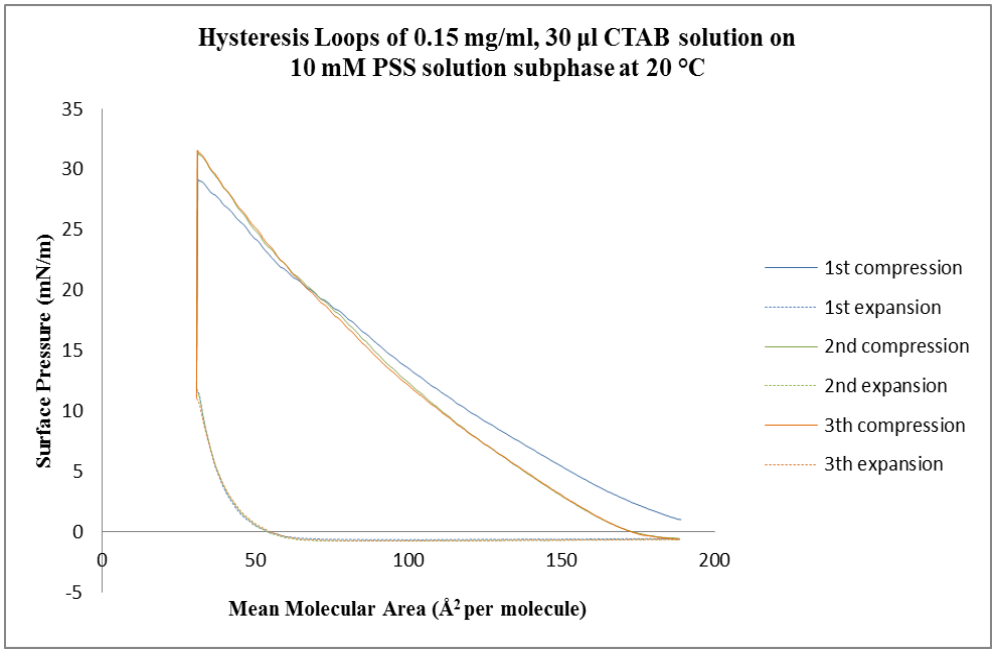

Figure 3. 24 Hysteresis loops of CTAB on 10mM PSS solution subphase, 0.15mg/ml CTAB solution in $CHCl_3$ at 20°C, it was waited for 5 min after 1st compression at target mean molecular area 10 $Å^2$/molecule (return target 46 $Å^2$/molecule)

Different from the initial hysteresis results, all compressions and all expansions were similar in their own for the compression-expansion cycles of CTAB obtained on 10mM PSS solution subphase. The surface pressure decreases distinctively for each expansion it can be seen from Figure 3.24.

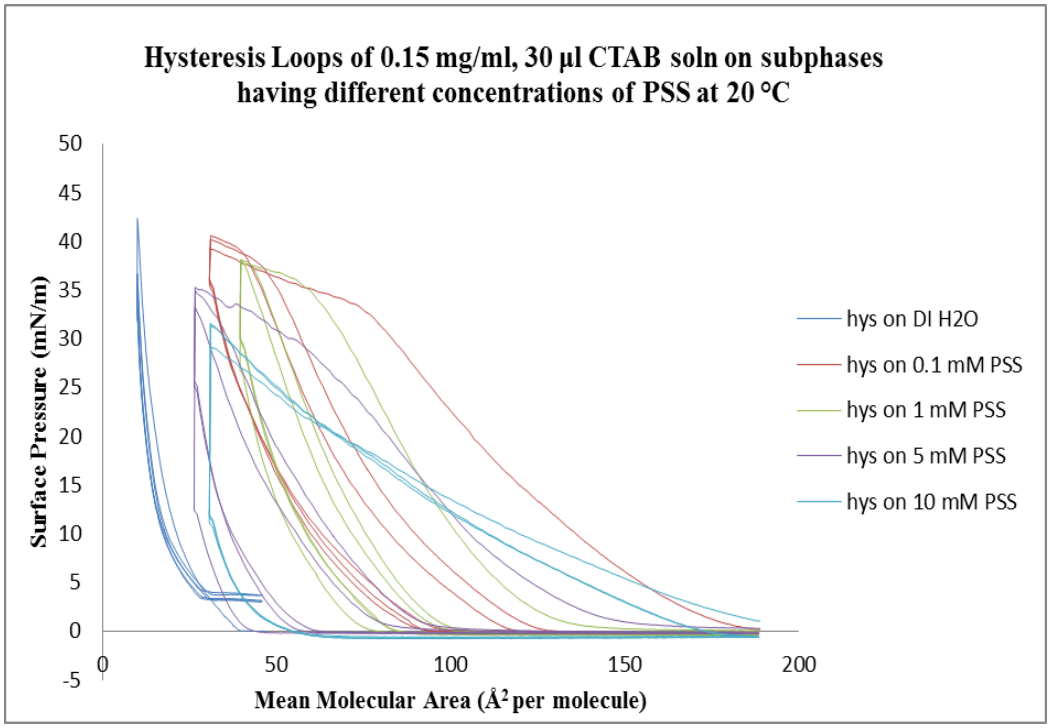

Figure 3. 25 Effect of PSS concentration in subphase on CTAB hysteresis loops, 0.15mg/ml CTAB solution in $CHCl_3$ at 20°C, it was waited for 5 min after 1st compression at target mean molecular area 10 $Å^2$/molecule (return target 46 $Å^2$/molecule)

Figure 3.25 represents the effect of PSS concentration in the subphase on the hysteresis loops of CTAB. Although it cannot be said there exists a regular increase in the surface pressure drop, presence of PSS affects the behavior of the molecules in the monolayer. In this part of the hysteresis experiments which based on waiting after compressions may not reflect the exact effect just caused by PSS. Compressing and holding monolayer at a target value may be challenging for the instrument. So in order to have an idea the experiments were repeated without waiting.

In this hysteresis study, it wasn`t waited between the cycles and the target value for compression was the minimum mean molecular area where the barriers were very close to the Wilhelmy plate and for the expansion, it was the maximum through area.

The matching of the first compression of hysteresis loops with the previously obtained isotherms was checked for each experiment. Results were represented below:

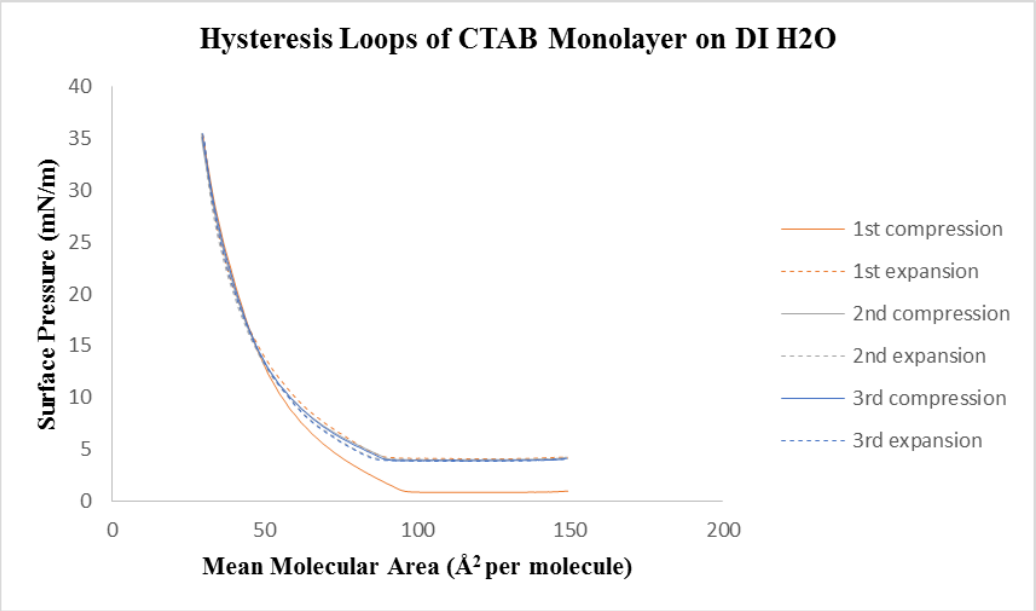

Figure 3. 26 Hysteresis loops of CTAB on DI H2O subphase, 0.15mg/ml CTAB solution in $CHCl_3$ at 20°C at target barrier position 72 mm (return target 0 mm)

It was obviously seen from the Figure 3.26, all the compression and expansions cycles intercepted to each other. This result implies that, on the DI H_2O subphase, molecules come together and go far from each other in a same way without any shift. The only difference apart from the first compression cycle was the earlier stabilization of gas phase at higher surface pressures.

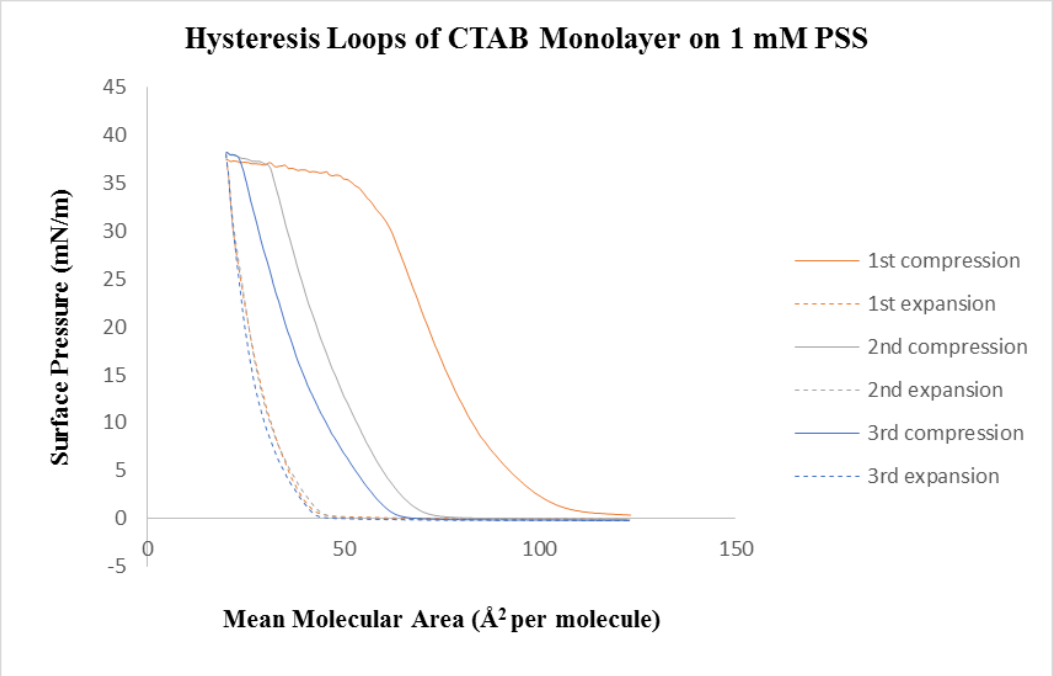

Figure 3. 27 Hysteresis loops of CTAB on 1mM PSS subphase, 0.15mg/ml CTAB solution in $CHCl_3$ at 20°C at target barrier position 72 mm (return target 0 mm)

Same experiment was repeated in the presence of the 1mM PSS solution subphase. According to obtained data illustrated in Figure 3.27, again a shift to the lower mean molecular areas was observed. Consistent with the previous isotherm results, collapse point was significant for each compression when PSS was added to the subphase.

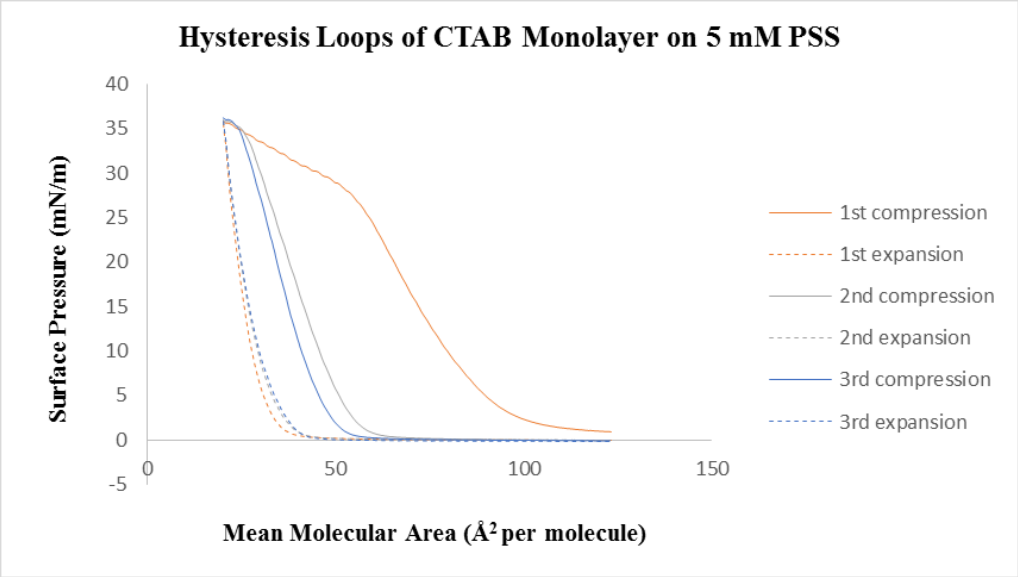

Figure 3. 28 Hysteresis loops of CTAB on 5mM PSS subphase, 0.15mg/ml CTAB solution in $CHCl_3$ at 20°C at target barrier position 72 mm (return target 0 mm)

Figure 3.28 represents the hysteresis curve when the CTAB molecules were compressed and expanded repeatedly. Again there exists a shift with the increase in the number of the cycles. The collapse point was distinctive just for the first compression and compared with the former experiment it was slightly recognized.

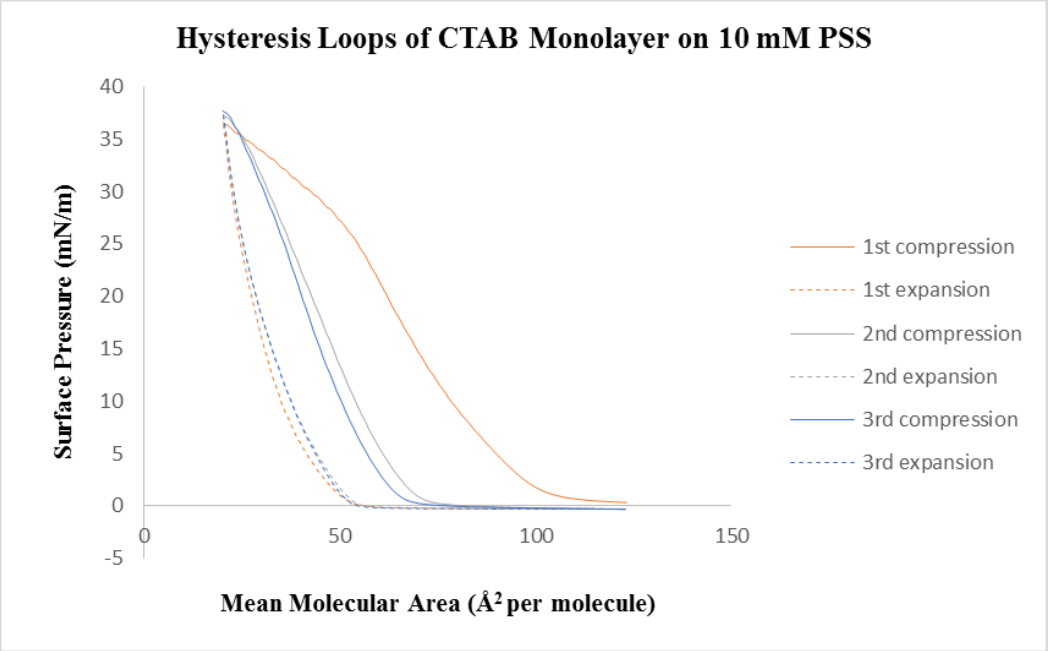

Figure 3. 29 Hysteresis loops of CTAB on 10mM PSS subphase, 0.15mg/ml CTAB solution in $CHCl_3$ at 20°C at target barrier position 72 mm (return target 0 mm)

In Figure 3.29 implies that the shift was smaller for 10mM compared with the other concentrations. Compressions and expansions were consistent in their own. All the hysteresis experiments without waiting after compressions were performed at target barrier position which was 72mm and the molecules were expanded completely. Since the compression was continued after the collapse point, for the exact decision of the effect of PSS amount on the monolayer stability, the experiments were repeated up to the collapse points where the monolayer was solid phase. For this aim, the hysteresis loops were obtain until the highest surface pressure value of the solid phase for compression and again the maximum trough area for the expansion to determine the effect of just PSS concentration in the subphase. For all hysteresis studies, to see a trend clearly, 3 compression and 3 expansion (6 cycles) were completed. To get reproducible results, the experiments were repeated several times

and matching of the isotherms with hysteresis lines was checked. Obtained data were shown following figures.

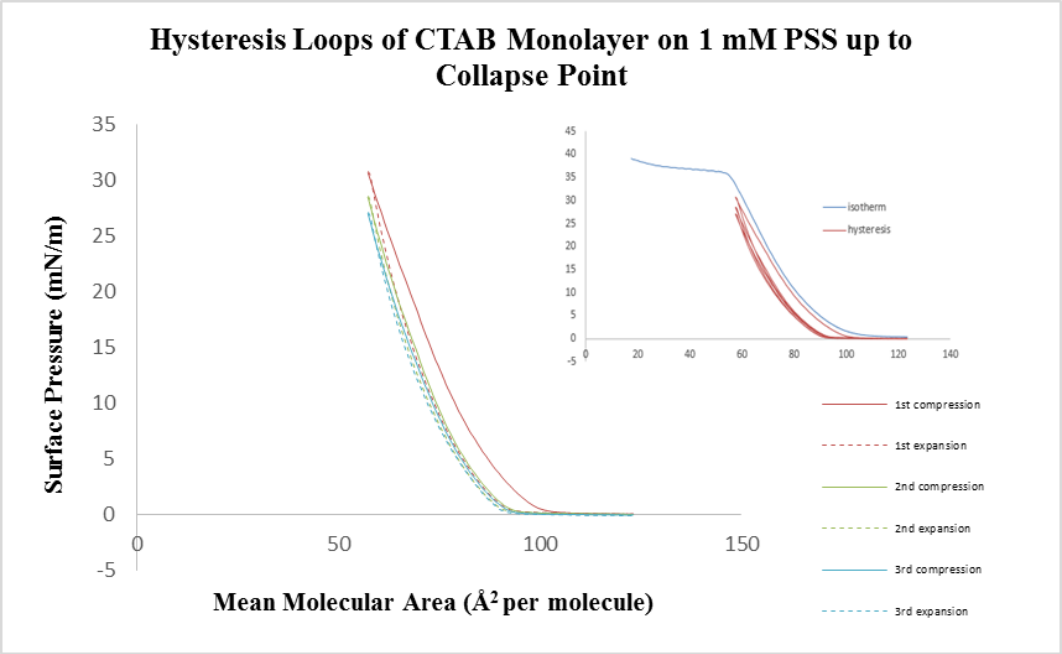

Figure 3. 30 Hysteresis loops of CTAB on 1mM PSS subphase, 0.15mg/ml CTAB solution in $CHCl_3$ at 20°C at target barrier position 55 mm (return target 0 mm) (inset hysteresis loops until the collapse point)

Figure 3.30 summaries the result recorded when the CTAB molecules were compressed and expanded on 1 mM PSS solution subphase up to the solid phase barrier position target. It can be said that there was a really small shift to the lower MMA and except from the first cycle, all curves were matching with each other. At the 2nd and 3rd compressions, the maximum surface pressure value decreases slightly.

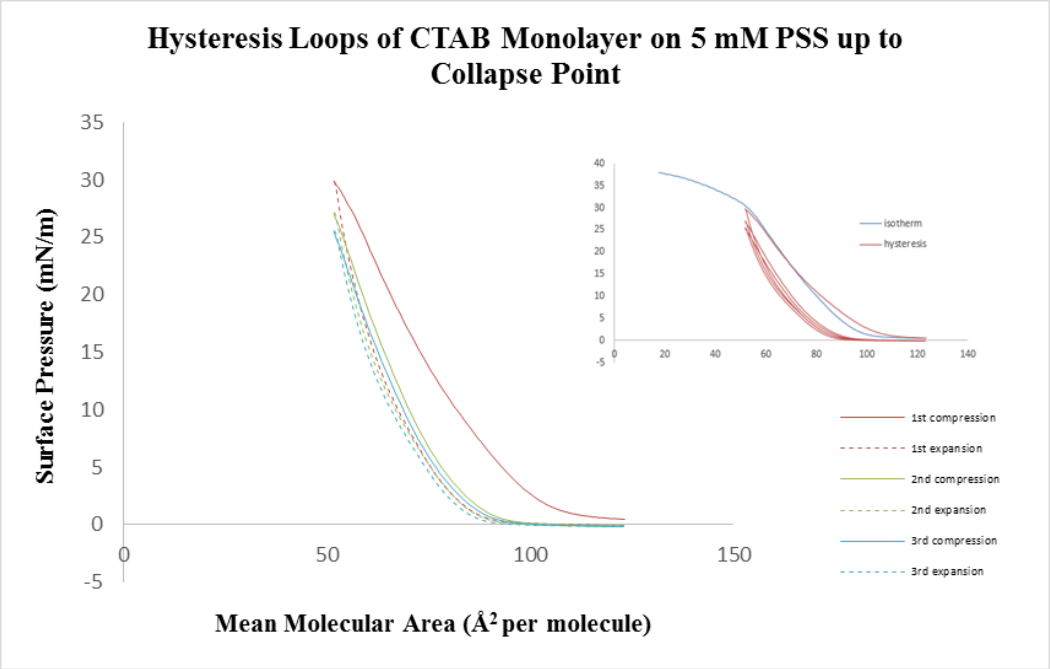

Figure 3. 31 Hysteresis loops of CTAB on 5mM PSS subphase, 0.15mg/ml CTAB solution in $CHCl_3$ at 20°C at target barrier position 50 mm (return target 0 mm) (inset hysteresis loops until the collapse point)

According to Figure 3.31, same explanations can be accepted for the 5mM PSS concentration. The main differences were a relatively larger shift in MMA and a larger drop in surface pressure in 2nd and 3rd loops compared with the data obtained in the previous 1mM PSS experiment.

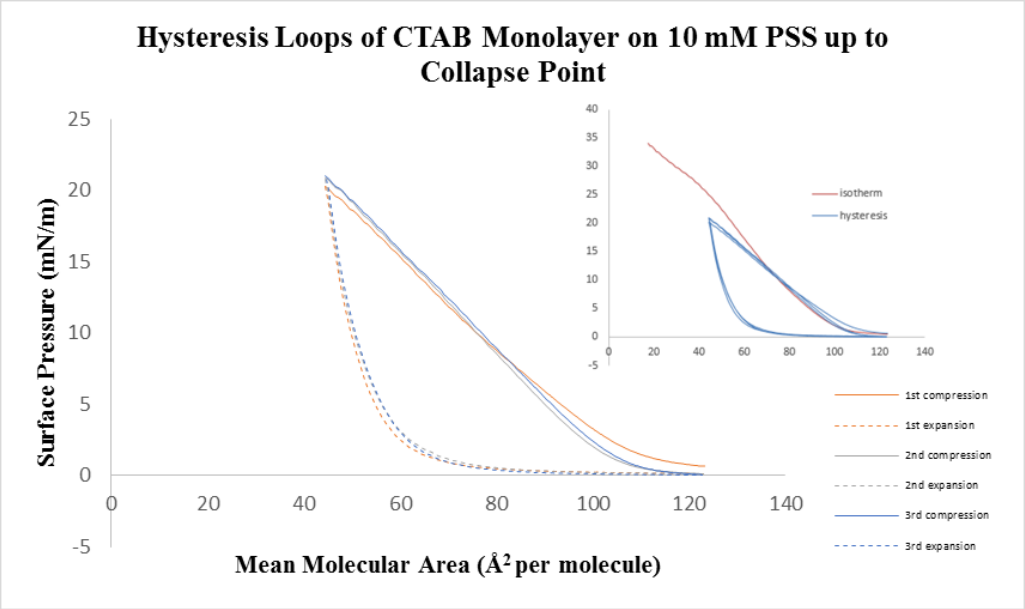

Figure 3. 32 Hysteresis loops of CTAB on 10mM PSS subphase, 0.15mg/ml CTAB solution in $CHCl_3$ at 20°C at target barrier position 53 mm (return target 0 mm) (inset hysteresis loops until the collapse point)

Figure 3.32 shows that CTAB molecules behaved in same way for all the compressions and they got far from each other similarly in all expansion cycles. A large shift was obtained just for the expansions. Compared with the other results, maximum surface pressure was relatively lower when the hysteresis loops were obtained on subphase having 10mM PSS.

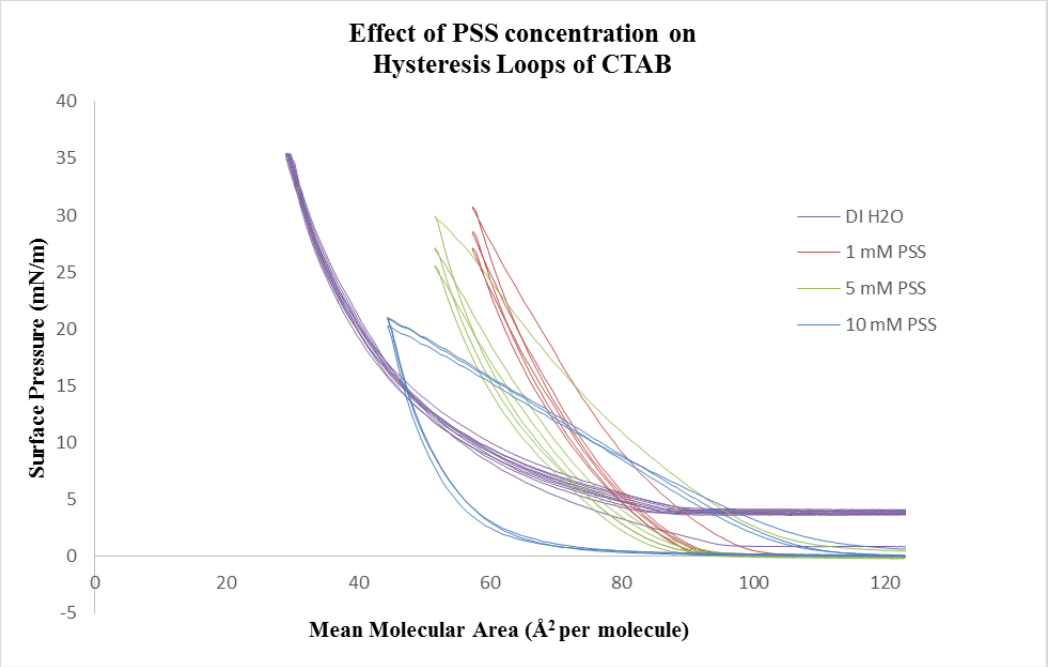

Figure 3. 33 Effect of PSS concentration in subphase on CTAB hysteresis loops, 0.15mg/ml CTAB solution in $CHCl_3$ at 20°C

Figure 3.33 shows the effect of PSS concentration on the hysteresis loops of CTAB clearly. The shifts in the curves to the lower mean molecular areas and the decreases in the surface pressures were directly related with the amount of PSS. By eliminating the errors may come from the instrument with the order of waiting at a specific target, the exact results that show only the effect of PSS were obtained. It can be concluded that, as the amount of PSS increases, the stabilization of the monolayer also increases. In order to strengthen this finding, the effect of PSS concentration on the efficiency of the transfer of CTAB monolayers was investigated.

3.3. Preparation of Gold Nanorod Monolayers

3.3.1. Synthesis of Gold Nanorods

Gold nanorods were synthesized with seed mediated growth method[43]. CTAB forms bilayer on the sides of rods[59] as seen in Figure 3.34. GNRs are composed of two orientation; (100) for the side faces and (111) for the tips of the rods. Since CTAB has a less affinity to (111) plane, the amount of CTAB on tips is less than at side faces.

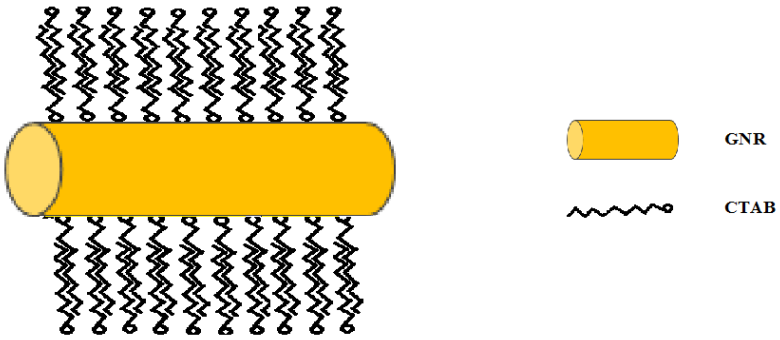

Figure 3. 34 Bilayer form of CTAB on GNRs

Figure 3.35 (**A** and **B**) and Figure 3.36 show the SEM images and the UV results of the synthesized GNRs, respectively.

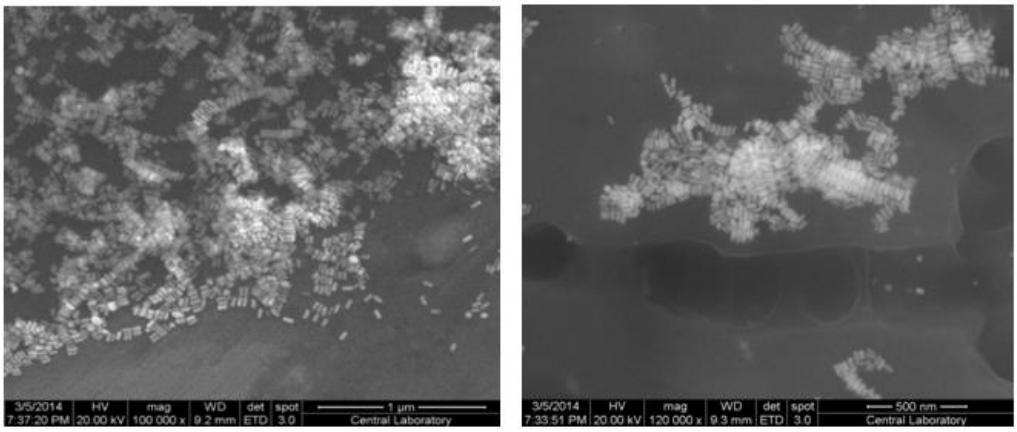

Figure 3. 35 SEM images of synthesized GNRs (**A** scale 1µm, **B** scale 500nm)

From the SEM images it can be seen that homogeneous, rod-like morphology of the gold was obtained. The aspect ratio of the rods were approximately 2.5. Alignment of GNRs is mostly parallel (side by side) to each other. GNRs in the solution can take any possible positions and orientations however as the concentration decreases by the evaporation of solvent, they align parallel to each other[60].

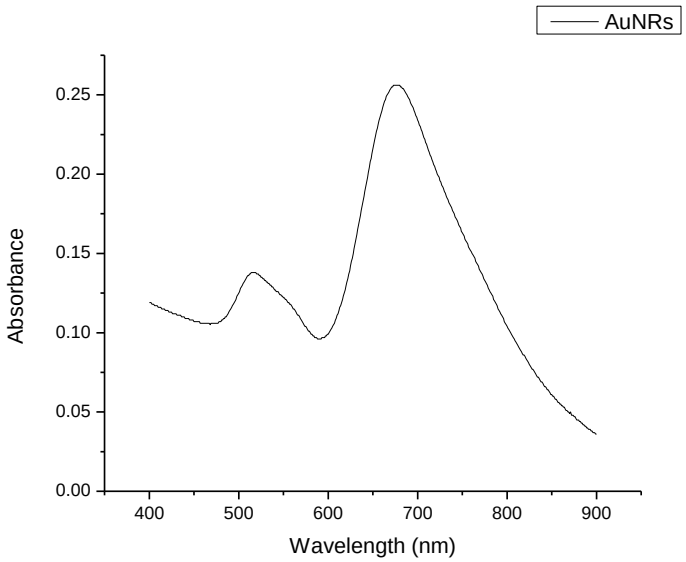

Figure 3. 36 UV-vis spectra of GNRs

UV result also confirm the rod like structure. There are two absorption bands at 520 and 675 nm corresponding to characteristic gold nanorods transverse and longitudinal plasmon absorptions respectively.

3.3.2. Surface Modification of Gold Nanorods

In order to convert the GNRs into Langmuir compatible form, the surface modification of GNRs were performed and they capped with ODT. After the treatment was completed, some amount of GNRs was added to chloroform to prove the surface modification. It is clearly seen from the Figure 3.37 that while the unmodified (CTAB capped) GNRs agglomerates, the ODT capped GNRs were well dispersed in chloroform.

Figure 3. 37 Image of CTAB capped GNRs (left), ODT capped GNRs (right) in chloroform media

The SEM images of the ODT capped GNRs were also represented in Figure 3.38 below.

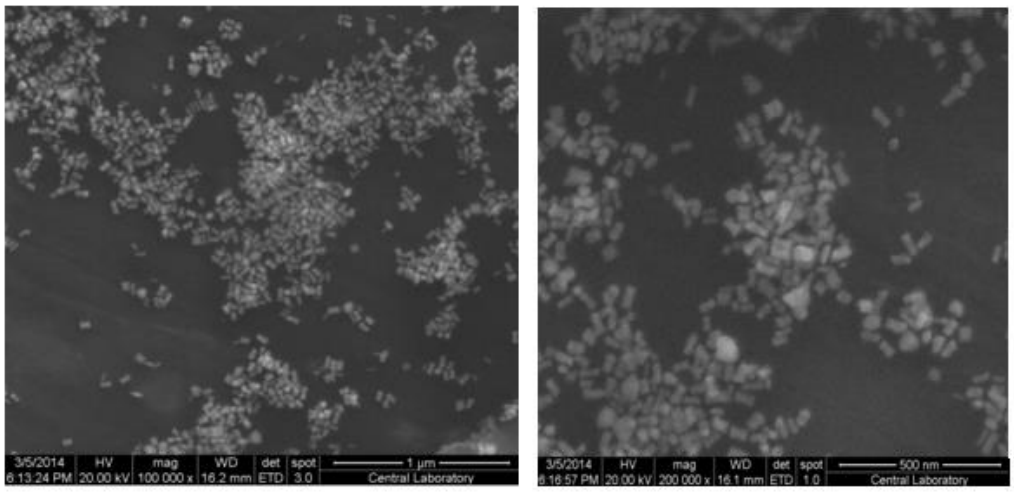

Figure 3. 38 SEM images of ODT capped GNRs (**A** scale 1µm, **B** scale 500 nm)

It is seen that, after the surface modification, the morphology of the GNRs was changed and they had dog bone like structure. The homogeneity of the structures

disappeared and the aspect ratio of the GNRs were also changed. Similar observation was reported by Lin and Chau, in the preparation of alkanthiolate gold nanorods for LB studies. According to the study, surface modification can result of the decrease in the aspect ratio of the rods due to the loss of the stability during the change and the tendency of rods to return sphere-like shape[44].

3.3.3. Preparation of ODT Capped GNR Films

Once the surface modification was completed, a very dilute solution of ODT capped hydrophobic GNRs was dispersed into chloroform. The prepared dilute solution was spread on the water subphase of LB system and monolayer of the ODT capped GNRs was tried to obtain. Figure 3.39 represents the isotherm of ODT capped GNRs on DI H_2O subphase.

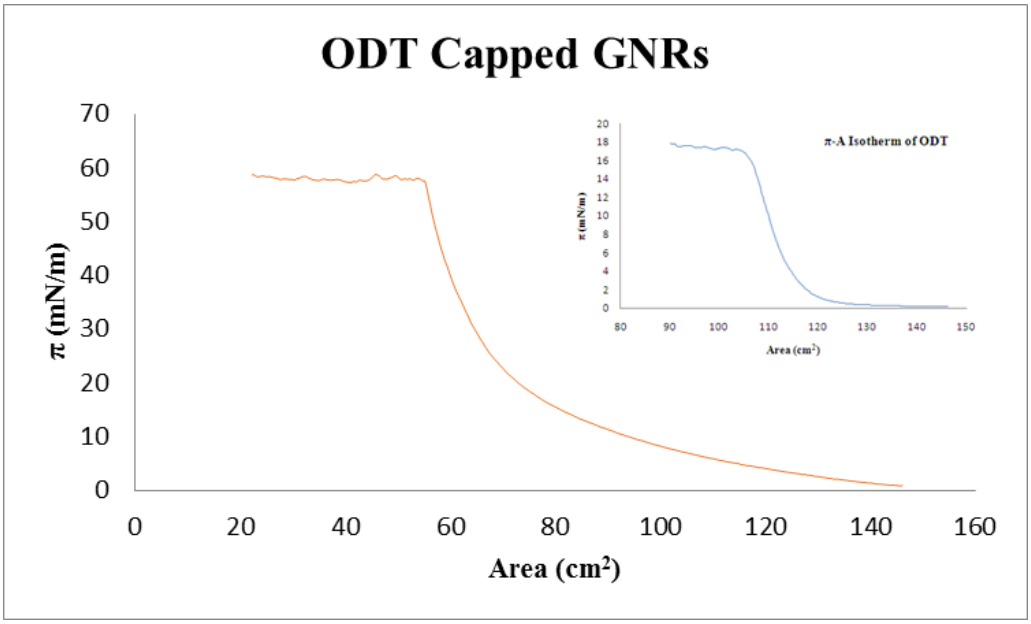

Figure 3. 39 π-A isotherms of 23 µl ODT capped GNR solution in $CHCl_3$ on DI H_2O subphase, 2.00 mg/ml ODT capped GNR solution at 20°C (inset π-A isotherms of ODT only)

It can be seen from the Figure 3.39, the phase transitions were obtained in π-A isotherms of the ODT capped GNRs and the collapse point was approximately at 60mN/m. The inset figure represents the π-A isotherms of the ODT only. When the isotherms of ODT capped GNRs and ODT were compared, both graphs represent almost same behavior except the difference in the surface pressures at collapse points. The collapse of ODT isotherm was at lower surface pressure value compared with ODT capped GNR isotherm. The SEM images of the transferred layer were represented in Figure 3.40.

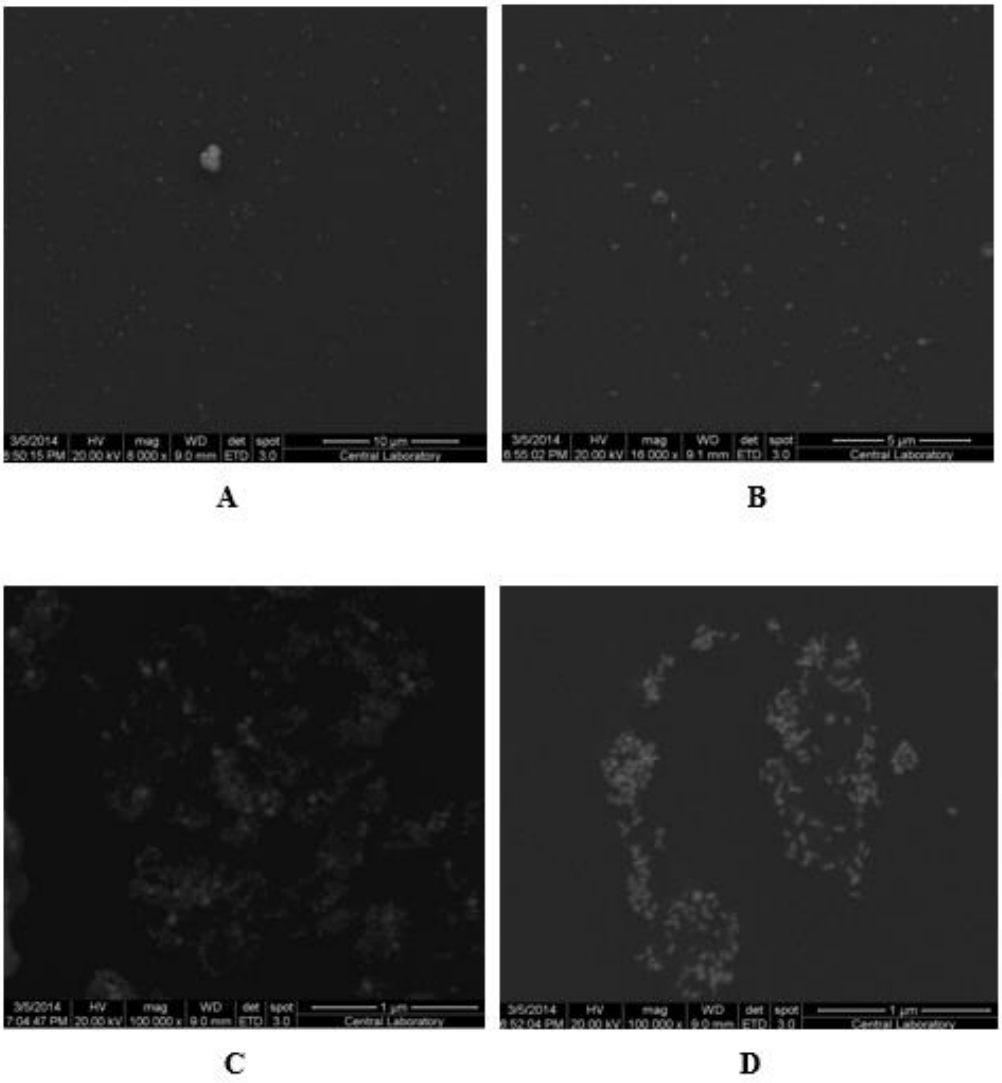

Figure 3. 40 SEM images of ODT capped GNR on solid support (**A** scale 10µm, **B** scale 5µm, **C** and **D** 1 µm)

It can be seen from the Figure 3.40, a homogeneous monolayer of GNRs could not be obtained although the TR was very close to 1 during the deposition. So, while the TR was implying that the transfer was done appropriately, the SEM results show that

ODT capped GNRs do not form a monolayer on the substrate. There are only few domains of GNRs. Therefore we concluded that the free ODT molecules, introduced into the solution together with the GNRs, formed a stable Langmuir monolayer on the solution. TR values close to one should be an indication of the successful transfer of ODT layer onto the substrate not the nanorod assembly. Since minute amount of ODT is enough for the monolayer formation, excess washing-centrifuging cycles following the surface modification do not remove them completely but disturb the morphology. On the other hand, although small amount of nanorods were transferred, they should have been transported by ODT monolayer through hydrophobic interactions in between ODT side chains of nanorods and LB layer. Therefore by altering the amount of the GNR, the volume of the chloroform and the evaporation conditions an appropriate GNR monolayer would be formed. Before starting further studies on this respect, the surface modification method, to render the surface of cationic gold nanorods hydrophobic, should be optimized which was out of the scope of this thesis. Therefore for the preparation of GNR assemblies we decided to use as prepared cationic nanorods.

3.4. Preparation of PSS Glued Multilayers

With the aim of multilayer preparation, it was continued with the transfers of obtained monolayers onto the solid support. Before deposition, hydrophobic treatment of substrate surface was performed. After the stabilization of CTAB monolayer on the surface, the dipping process was initiated. Figure 3.41 represents the transfer of monolayer and the surface pressure as a function of time. As the substrate is lifted the monolayer is transferred onto the solid support and the amount of surfactant on the subphase surface decreases. Thus the surface pressure decreases and the barriers move closer together to compensate causing the sinusoidal behavior of the surface pressure curve.

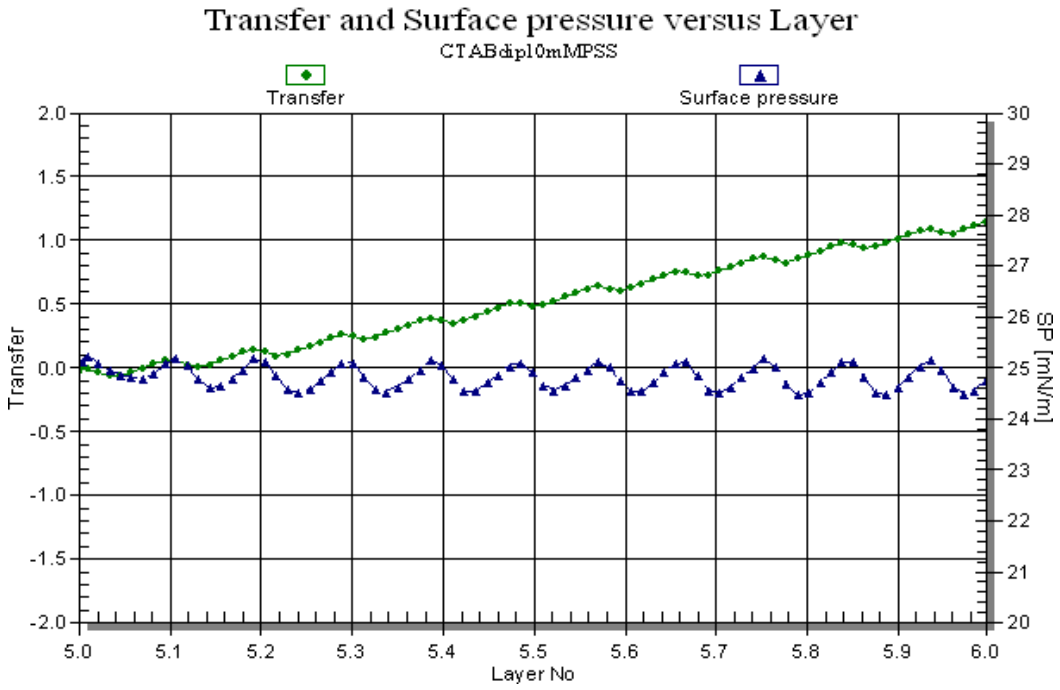

Figure 3. 41 Transfer and surface pressure trend vs layer no graph displaying the deposition of a CTAB monolayer onto a substrate from the surface of 10mM PSS solution subphase

It can be seen from Figure 3.41, CTAB monolayer on the surface could be hold stable at the target surface pressure in the presence of 10mM PSS in the subphase. Table 3.3 represents the TR results of the CTAB multilayer preparation.

Table 3. 3 Transfer ratio results of CTAB multilayer from the surface of 10mM PSS solution subphase

Layer no	Direction	Total TR
1	Up	1.585
2	Down	1.506

Table 3. 3 (continued)

3	Up	-0.326

It can be seen from the Table 3.3, PSS glued CTAB multilayers having 6 layers can be obtained. TR results of the some layers were not ideal but as mentioned before, for the deposition experiments, some parameters should be optimized and so in the further studies, the efficiency of the transfers will be improved.

3.5. Application of PSS Glued CTAB Films as SERS Substrate

Prepared PSS glued CTAB monolayers was used as a surface enhanced raman spectroscopy (SERS) substrate.

3.5.1. Surface Enhanced Raman Spectroscopy

The effect of the PSS on the stabilization of CTAB monolayers and improved strength of the attachment of these PSS stabilized CTAB monolayers with the GNRs were investigated by comparing the intensity of Raman signals of BCB. After the transfer of CTAB monolayer both absence and the presence of PSS in the subphase, the substrate was touched GNR solution surface and waited for 5 minutes to improve the attachment of rods appropriately and let it dry. Enhancement of the signal intensity of an organic dye which is BCB (brilliant crystal blue) on the prepared substrates was compared. Results were summarized with the below figures.

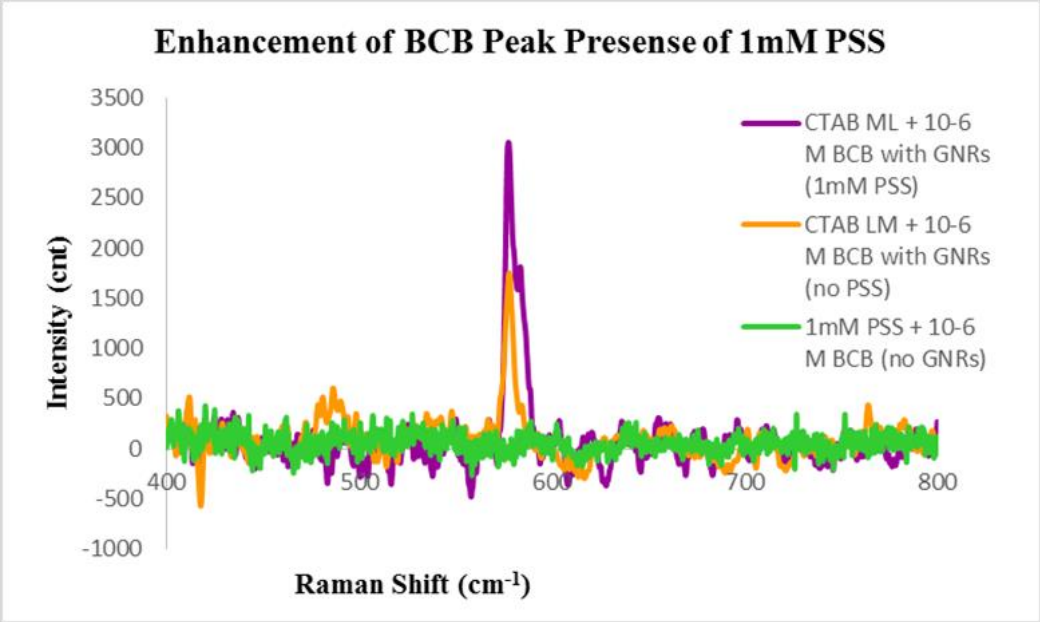

Figure 3. 42 Raman spectra of 1 mM PSS stabilized CTAB monolayer + 10^{-6} M BCB (with GNRs), CTAB monolayer + 10^{-6} M BCB (no PSS) and 1mM PSS stabilized CTAB monolayer + 10^{-6} M BCB (no GNRs)

Figure 3.42 shows the enhancement of the BCB peak with the addition of PSS into the subphase. It can be said that the performance of the CTAB monolayer transferred from the 1mM PSS subphase as a SERS substrate is greater than the performance of the monolayer deposited from the DI H_2O surface. At the presence of the PSS, positively charged CTAB bilayer capped GNRs attaches effectively to the substrate surface. To see the effect of PSS concentration on this attachment, experiments were repeated with the substrates prepared by transferring from different amounts of PSS solution subphases.

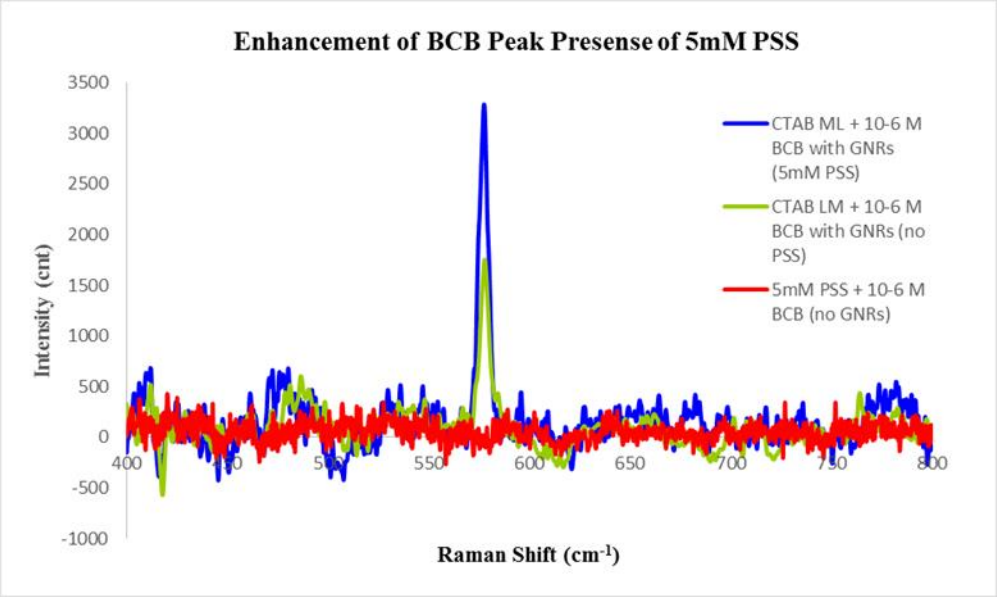

Figure 3. 43 Raman spectra of 5 mM PSS stabilized CTAB monolayer + 10^{-6} M BCB (with GNRs), CTAB monolayer + 10^{-6} M BCB (no PSS) and 5 mM PSS stabilized CTAB monolayer + 10^{-6} M BCB (no GNRs)

The enhancement of the BCB peak with 5 mM PSS was represented in Figure 3.43. Same explanations can be done for this result also.

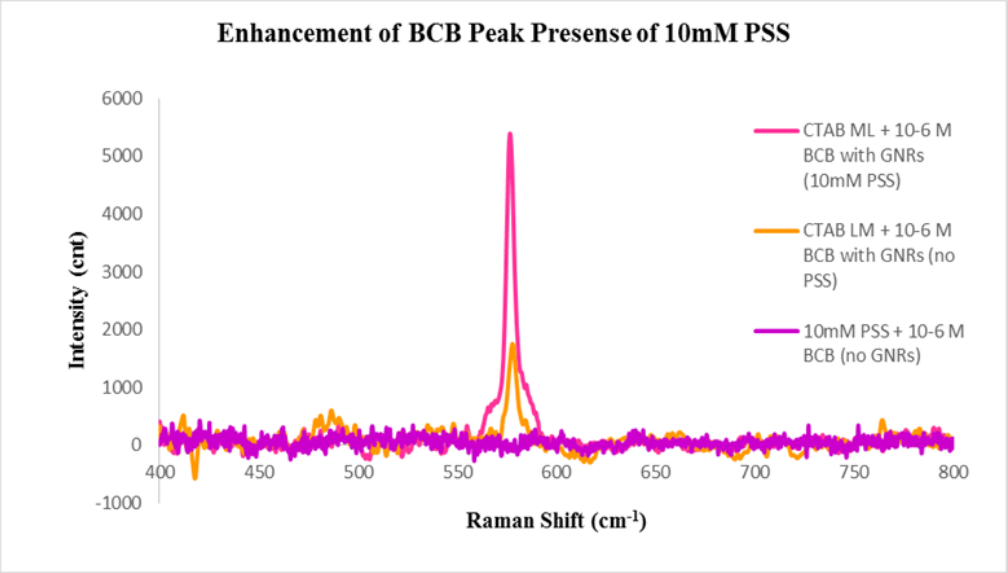

Figure 3. 44 Raman spectra of 10 mM PSS stabilized CTAB monolayer + 10^{-6} M BCB (with GNRs), CTAB monolayer + 10^{-6} M BCB (no PSS) and 10 mM PSS stabilized CTAB monolayer + 10^{-6} M BCB (no GNRs)

For the final study, the experiment was performed in the presence of 10 mM PSS. According to Figure 3.44, the highest enhancement was obtained with this concentration. In order to distinct the effect of PSS concentration on the enhancement, the results were shown in the same graph.

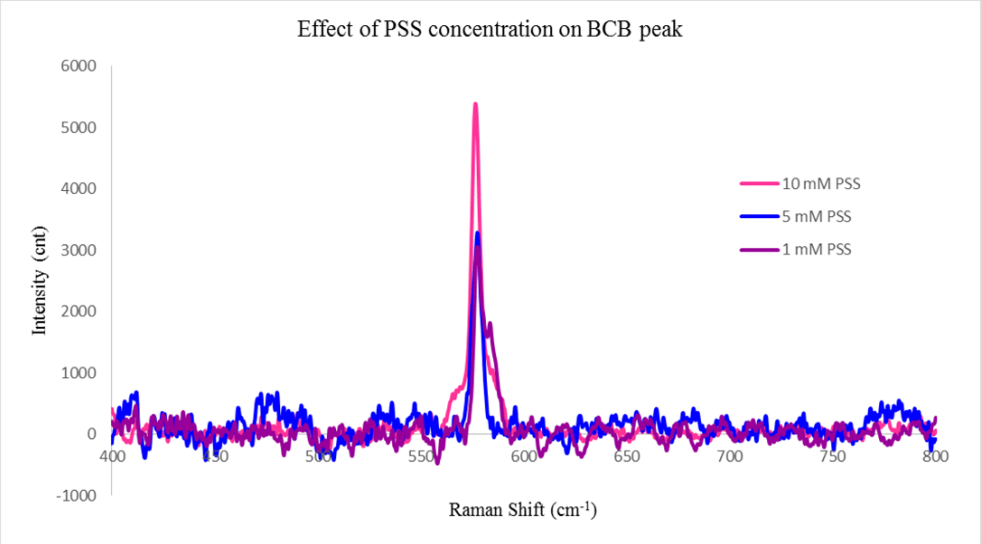

Figure 3. 45 Effect of PSS concentration in subphase where CTAB monolayer transferred from on enhancement of 10^{-6} M BCB peak with GNRs

Figure 3.45 shows the effect of PSS on the BCB peak enhancement clearly. It can be concluded that, there was a small difference between the performances of the substrates which were prepared by transferring the CTAB monolayer from the surface of both 1 and 5 mM PSS solution subphase. On the other hand, the amount of PSS was increased, the enhancement was obtained higher. So increase in the PSS concentration in the subphase leads to stronger attachment with the GNRs as a more sensitive substrates. In the study, SERS also provides a proof of the presence of PSS on the surfaces.

In the further studies, for the efficient interaction of the GNRs with PSS, waiting time of the substrate on the GNR solution surface will be increased.

CHAPTER 4

CONCLUSION

Organic thin films with their wide range application areas have a great importance due to their tunable properties by changing their assembly. Preparation and deposition of such films in a highly controllable way with Langmuir and Langmuir Blodgett techniques provide new opportunities for the researchers in this field.

In this study, highly stable, water soluble CTAB monolayers were prepared without using complex formation with another insoluble material at the air-water interface by Langmuir technique. In order to obtain efficient transfers of the prepared monolayers onto solid supports, some critical parameters such as temperature and pH of the subphase, concentration of spreading solution, compression rate of barriers and transfer rate of the dipping arm were optimized with the standard materials which are SA and ODT. Similar optimizations were performed with CTAB initially because the further aim of the study was to prepare and organize the gold nanorods in a monolayer structure. After determination of the optimum parameters to obtain high quality films, the factors that affect the stability of the CTAB monolayers were investigated. To improve the stability of the films and the transfer of them, gluing approach that based on the addition of oppositely charged polyelectrolyte into subphase was added. Poly(4-styrenesulfonate) (PSS) was used as a gluing agent. In order to compare the effect of PSS on stability of the obtained monolayers, hysteresis experiments were performed in the presence and absence of PSS in the subphase. It was determined that increase in the concentration of the PSS in the subphase resulted in the change in the behavior of the CTAB molecules when they were compressed and expanded repeatedly. As expected, there is a hysteresis in the presence of PSS in

the subphase. The presence of polymer layer on the surface keeps CTAB molecules attached to each other during expansion.

The quality of the depositions of glued and unglued monolayers were compared and it was recognized that, CTAB itself already can be transferred onto a substrate surface ideally and the gluing is not a requirement to obtain stable CTAB multilayers. The important point is that, LB multilayers of CTAB-PSS layers were obtained, by alternately deposition of PSS and CTAB on the substrate, successfully.

Gold nanorods were prepared using seed mediated growth approach, their surfaces were made hydrophobic and their plasmon properties were examined to confirm the quality of nanorods together with the SEM measurements.

Au nanorod layer was constructed on the CTMS-functionalized glass substrate using glued CTAB LB technique. The negatively charged polyelectrolyte PSS was used as a glue molecule of the interlayer Au nanorods.

After the deposition of PSS stabilized CTAB monolayers, the performance of the obtained structures as Surface Enhanced Raman Scattering (SERS) substrates were investigated using brilliant cresyl blue (BCB) as a probe. It was concluded that the presence of the PSS during the deposition of the CTAB monolayers leads to stronger attachment with the gold nanorods providing an enhancement in the intensity of the BCB dye. In future several gold nanorod layers will be packed on the same substrate using the same strategy to achieve high coverage density of gold nanorods on the surface.

As a future work, the effect of different types of polyelectrolytes on the stabilization of the films and the membrane properties of the prepared films will be investigated. The efficiency of the gluing on the monolayers of the surfactants having shorter chains will be examined. With the help of the obtained findings about CTAB in this study, orientation and the film properties of GNRs will be studied.

REFERENCES

1. Rajca, A. An Introduction To Ultrathin Organic Films: From Langmuirblodgett To Self-Assembly, By Abraham Ulman, Academic Press, London 1991, Xxiii, 442Pp., $65, ISBN 0-12-708230-1. *Adv. Mater.* **4,** 309–309 (1992).

2. Devaux, H. Dünne Lamellen und ihre physikalischen Eigenschaften. *Kolloid-Zeitschrift* **58,** 260–276 (1932).

3. Langmuir-Blodgett Films. at <http://download.springer.com/static/pdf/156/bok%253A978-1-4899-3716-2.pdf?auth66=1422009348_b9ff73c8cb389a0f96d1e24d5871abcb&ext=.pdf> [last accessed on 2015-01-23]

4. Barnes, G. & Gentle, I. *Interfacial Science: An Introduction*. 325 (Oxford University Press, 2011). at <https://books.google.com/books?id=2XWcAQAAQBAJ&pgis=1> [last accessed on 2015-01-29]

5. Petty, M. C. *Langmuir-Blodgett Films: An Introduction*. 234 (Cambridge University Press, 1996). at <https://books.google.com/books?id=qCk-2S_VKugC&pgis=1> [last accessed on 2015-01-29]

6. *Insoluble monolayers at liquid-gas interfaces*. (1966). at <https://books.google.com/books?id=MU9OAQAAIAAJ&pgis=1> [last accessed on 2015-01-29]

7. Matharu, Z., Bandodkar, A. J., Gupta, V. & Malhotra, B. D. Fundamentals and application of ordered molecular assemblies to affinity biosensing. *Chem. Soc. Rev.* **41,** 1363 (2012).

8. Smith, R. K., Lewis, P. a & Weiss, P. S. Patterning self-assembled monolayers. *Prog. Surf. Sci.* **75,** 1–68 (2004).

9. a new approach to generate thiol terminated SAMs on gold. at <https://www.toyo.co.jp/file/pdf/spm/files/agi/5989-7699EN.pdf> [last accessed on 2015-01-23]

10. Hussain, S. A., Deb, S. & Bhattacharjee, D. Langmuir-Blodgett technique a unique tool for fabrication of Ultrathin Organic Films . Abstract : History of Langmuir-Blodgett (LB) films : LB compatible material : **4,** 1–8 (2005).

11. Osvaldo, N. & Oliveira, J. Langmuir-Blodgett Films - Properties and Possible Applications. *Brazilian J. Phys.* **22,** 60–69 (1992).

12. Deb, S., Biswas, S., Hussain, S. a. & Bhattacharjee, D. Spectroscopic characterizations of the mixed Langmuir-Blodgett (LB) films of 2,2???-biquinoline molecules: Evidence of dimer formation. *Chem. Phys. Lett.* **405,** 323–329 (2005).

13. Acharya, S., Bhattacharjee, D., Sarkar, J. & Talapatra, G. . Spectroscopic study of non-amphiphilic 2-(4-biphenylyl)-5-(4-tert-butylphenyl)-l,3,4-oxadiazole aggregates at air–water interface and in Langmuir–Blodgett films. *Chem. Phys. Lett.* **393,** 1–6 (2004).

14. Acharya, S., Bhattacharjee, D. & Talapatra, G. B. Spectroscopic study of non-amphiphilic 9-phenyl fluorene assembled in Langmuir-Blodgett films in two different matrices: Dimer and excimer formation. *Chem. Phys. Lett.* **372,** 97–103 (2003).

15. Vitukhnovsky, A. G., Sluch, M. I., Warren, J. G. & Petty, M. C. The fluorescence of perylene-doped Langmuir—Blodgett films. *Chem. Phys. Lett.* **173,** 425–429 (1990).

16. Ferreira, M. *et al.* Preparation, characterization and taste sensing properties of Langmuir–Blodgett Films from mixtures of polyaniline and a ruthenium complex. *Polymer (Guildf).* **44,** 4205–4211 (2003).

17. Ferreira, M., Dinelli, L. R., Wohnrath, K., Batista, A. a. & Oliveira, O. N. Langmuir-Blodgett films from polyaniline/ruthenium complexes as modified electrodes for detection of dopamine. *Thin Solid Films* **446,** 301–306 (2004).

18. Models, A. Software Manual Langmuir and Langmuir-Blodgett devices. 0–103

19. Kaganer, V., Möhwald, H. & Dutta, P. Structure and phase transitions in Langmuir monolayers. *Rev. Mod. Phys.* **71,** 779–819 (1999).

20. Israelachvili, J. Self-Assembly in Two Dimensions: Surface Micelles and Domain Formation in Monolayers. *Langmuir* **10,** 3774–3781 (1994).

21. Fainerman, V. B., Miller, R. & Wüstneck, R. Adsorption of Proteins at Liquid/Fluid Interfaces. *J. Colloid Interface Sci.* **183,** 26–34 (1996).

22. Kumaki, J., Kajitani, T., Nagai, K., Okoshi, K. & Yashima, E. Visualization of polymer chain conformations in amorphous polyisocyanide Langmuir-

Blodgett films by atomic force microscopy. *J. Am. Chem. Soc.* **132,** 5604–6 (2010).

23. Srivastava, S., Leiske, D., Basu, J. K. & Fuller, G. G. Interfacial shear rheology of highly confined glassy polymers. *Soft Matter* **7,** 1994 (2011).

24. Pohjakallio, M., Aho, T., Kontturi, K. & Kontturi, E. Morphology of poly(methyl methacrylate) and polystyrene blends upon Langmuir–Schaefer deposition. *Soft Matter* **7,** 743 (2011).

25. Li, J., Janout, V. & Regen, S. L. Glued Langmuir-Blodgett Film: An Unexpected Dependency of Gluing on Polyelectrolyte Concentration. *Langmuir* **20,** 2048–2049 (2004).

26. Regen, S. L. Porous and Glued Langmuir-Blodgett Membranes.

27. Wang, M., Janout, V. & Regen, S. L. Minimizing Defects in Polymer-Based Langmuir- Blodgett Monolayers and Bilayers Via Gluing S u p p o r t i n g I n f o r m a t i o n. 1–4

28. Li, J., Janout, V. & Regen, S. L. Gluing Langmuir - Blodgett Monolayers onto Hydrocarbon Surfaces. **7,** 682–683 (2006).

29. Li, J., Janout, V. & Regen, S. L. Sticky monolayers and defect-free Langmuir-Blodgett bilayers using poly(acrylamide) glue. *Chem. Mater.* **18,** 5065–5069 (2006).

30. McCullough, D. H., Grygorash, R., Hsu, J. T. & Regen, S. L. Insight into the permeation barrier of glued Langmuir-Blodgett bilayers. *J. Am. Chem. Soc.* **129,** 8663–8667 (2007).

31. Li, J., Janout, V. & Regen, S. L. Covalent gluing and postgluing of langmuir-blodgett monolayers at hydrocarbon surfaces. *Langmuir* **22,** 11224–11229 (2006).

32. Paul, S. *et al.* Langmuir−Blodgett Film Deposition of Metallic Nanoparticles and Their Application to Electronic Memory Structures. *Nano Lett.* **3,** 533–536 (2003).

33. Brust, M. *et al.* Langmuir−Blodgett Films of Alkane Chalcogenide (S,Se,Te) Stabilized Gold Nanoparticles. *Nano Lett.* **1,** 189–191 (2001).

34. Patil, V., Malvankar, R. B. & Sastry, M. Role of Particle Size in Individual and Competitive Diffusion of Carboxylic Acid Derivatized Colloidal Gold

Particles in Thermally Evaporated Fatty Amine Films. *Langmuir* **15,** 8197–8206 (1999).

35. Chen, L.-H., Dudek, A., Lee, Y.-L. & Chang, C.-H. Adsorption of carboxylate-modified gold nanoparticles on an octadecylamine monolayer at the air/liquid interface. *Langmuir* **23,** 3123–7 (2007).

36. Sastry, M. *et al.* Organization of polymer-capped platinum colloidal particles at the air–water interface. *Thin Solid Films* **324,** 239–244 (1998).

37. Swami, A., Kumar, A., Selvakannan, P., Mandal, S. & Sastry, M. Langmuir–Blodgett films of laurylamine-modified hydrophobic gold nanoparticles organized at the air–water interface. *J. Colloid Interface Sci.* **260,** 367–373 (2003).

38. Tao, A. *et al.* Langmuir-Blodgett silver nanowire monolayers for molecular sensing using surface-enhanced Raman spectroscopy. *Nano Lett.* **3,** 1229–1233 (2003).

39. Tao, A. R., Huang, J. & Yang, P. Langmuir-Blodgettry of nanocrystals and nanowires. *Acc. Chem. Res.* **41,** 1662–1673 (2008).

40. Jeong, D. H., Zhang, Y. X. & Moskovits, M. Polarized surface enhanced Raman scattering from aligned silver nanowire rafts. *J. Phys. Chem. B* **108,** 12724–12728 (2004).

41. Ling, X. Y. *et al.* Alumina-coated Ag nanocrystal monolayers as surfaceenhanced Raman spectroscopy platforms for the direct spectroscopic detection of water splitting reaction intermediates. *Nano Res.* **7,** 132–143 (2013).

42. Zhou, M. Y. *et al.* Effects of surface wettability and roughness of microchannel on flow behaviors of thermo-responsive microspheres therein during the phase transition. *J. Colloid Interface Sci.* **336,** 162–170 (2009).

43. Nikoobakht, B. & El-Sayed, M. a. Preparation and growth mechanism of gold nanorods (NRs) using seed-mediated growth method. *Chem. Mater.* **15,** 1957–1962 (2003).

44. Lin, C. & Chau, L. Langmuir-Blodgett films of alkanethiolate gold nanorods. *Journal-Chinese …* 1015–1021 (2003). at <http://proj3.sinica.edu.tw/~chem/servxx6/files/paper_7870_1269277625.pdf> [last accessed on 2015-01-23]

45. Islam, M. N. & Kato, T. Influence of temperature and alkyl chain length on phase behavior in Langmuir monolayers of some oxyethylenated nonionic surfactants. *J. Colloid Interface Sci.* **294,** 288–294 (2006).

46. *Surfactant Science and Technology: Retrospects and Prospects*. 593 (CRC Press, 2015). at <https://books.google.com/books?id=fF3NBQAAQBAJ&pgis=1> [last accessed on 2015-01-24]

47. Gupta, R. K., Suresh, K. a, Guo, R. & Kumar, S. Langmuir-Blodgett films of octadecanethiol--properties and potential applications. *Anal. Chim. Acta* **568,** 109–118 (2006).

48. Biswas, S., Bhattacharjee, D., Nath, R. K. & Hussain, S. a. Formation of complex Langmuir and Langmuir-Blodgett films of water soluble rosebengal. *J. Colloid Interface Sci.* **311,** 361–367 (2007).

49. Berg, J. M. & Eriksson, L. G. T. Mixed Monolayers and Langmuir-Blodgett Films Consisting of a Fatty Amine and a Bipolar Substance. *Langmuir* **10,** 1213–1224 (1994).

50. Gayathri, S. S. & Patnaik, A. Interfacial behaviour of brominated fullerene (C60Br24) and stearic acid mixed Langmuir films at air–water interface. *Chem. Phys. Lett.* **433,** 317–322 (2007).

51. Asnacios, A., Langevin, D. & Argillier, J.-F. Complexation of Cationic Surfactant and Anionic Polymer at the Air−Water Interface. *Macromolecules* **29,** 7412–7417 (1996).

52. Corkill, J. M., Goodman, J. F., Harrold, S. P. & Tate, J. R. Monolayers formed by mixtures of anionic and cationic surface-active agents. *Trans. Faraday Soc.* **63,** 247 (1967).

53. Tah, B., Pal, P., Mahato, M. & Talapatra, G. B. Aggregation behavior of SDS/CTAB catanionic surfactant mixture in aqueous solution and at the air/water interface. *J. Phys. Chem. B* **115,** 8493–9 (2011).

54. Sepirlveda, L. & Cortes, J. v n l Ionization Degrees and Crltical Micelle Concentrations of Hexadecyltrimethylammonium and TetradecyCtrimethylammonlum Micelles wlth Different Counterlons. **2,** 5322–5324 (1985).

55. Wang, M., Janout, V. & Regen, S. L. Minimizing defects in polymer-based Langmuir-blodgett monolayers and bilayers via gluing. *Langmuir* **28,** 4614–4617 (2012).

56. Li, J., Janout, V. & Regen, S. L. Covalent gluing and postgluing of langmuir-blodgett monolayers at hydrocarbon surfaces. *Langmuir* **22,** 11224–11229 (2006).

57. Sudheesh, S., Ahmad, J. & Singh, G. S. Hysteresis of Isotherms of Mixed Monolayers of N-Octadecyl-N′-phenylthiourea and Stearic Acid at Air/Water Interface. *ISRN Phys. Chem.* **2012,** 1–6 (2012).

58. Sudheesh, S. & Ahmad, J. Effect of wilhelmy plate material on hysteresis of langmuir film isotherms. *Asian J. Chem.* **25,** 3535–3538 (2013).

59. Gao, J., Bender, C. M. & Murphy, C. J. Dependence of the Gold Nanorod Aspect Ratio on the Nature of the Directing Surfactant in Aqueous Solution. *Langmuir* **19,** 9065–9070 (2003).

60. Ng, K. C. *et al.* Free-standing plasmonic-nanorod superlattice sheets. *ACS Nano* **6,** 925–934 (2012).